

## M4 BEAMLINE RADIATION PARAMETERS DUE TO NORMAL BEAM LOSS ON US COLLIMATOR 907

### Abstract

A description of work to estimate radiation parameters for normal beam loss on the 907 collimator at the M4 shielding berm, downstream of the M5 shield wall, and other points of interest is the subject of this document.

Leveling RPC, LLC  
6/17/19

## Contents

Introduction .....	3
The M4 Beamline Model .....	4
907 Collimator region model .....	4
M5 shield wall region.....	10
Particle splitting .....	13
MARS Simulation .....	14
Simulation results .....	14
Prompt Effective Dose Rate Histograms .....	14
Tissue Equivalent Detectors .....	24
Residual dose rate on collimator .....	26
Air Activation .....	27
Groundwater activation.....	29
Surface water activation .....	31
TLM detector system response .....	32
Analysis and Discussion .....	33
Supplemental shielding .....	36
Summary .....	36
References .....	36

## Introduction

The M4 beam line has been constructed with a nominal earth equivalent shielding thickness of 16 feet. At the time the Preliminary Shielding Assessment [2] was prepared, it was believed that significant beam losses throughout the M4 beam line would be minimal. The 16 foot earth equivalent shield was (and is) intended to be supplemented by active radiation detectors, in particular, Total Loss Monitoring systems (TLMs).

At the time of the Preliminary Shielding Assessment preparation, the mu2e experiment extinction system design requirements were under development. Subsequently, the extinction system has been advanced and now includes a collimator which has been positioned in the M4 beam line at 907 near the upstream end of the M4 beam line. The fraction of nominal beam loss at the 907 collimator is estimated to be about 0.3% of the 8 kW, 8 GeV proton beam, or about 24 watts [16]. The introduction of intentional beam loss at 8 GeV creates a significant challenge to the 16' shielding. In addition, the dynamic range of the TLMs planned for use in the M4 beamline tunnel could be exceeded by such a beam loss at the 907 collimator. Beam losses at the 907 collimator could result in production and release of significant air activation at the M4 beam line air exhaust duct located at the upstream end of the M4 beam line tunnel. Finally, beam losses in the upstream M4 line have the potential to present a beam-on radiation exposure situation downstream of the shield wall separating the M5 tunnel from the muon g-2 storage ring room.

The purpose of this document is to describe results of MARS [1] simulations is to:

- obtain prompt radiation dose rate estimates:
  - on the M4 shielding berm above the 907 collimator and downstream quadrupoles Q908 and Q909
  - at the nearby exit stairway door
  - downstream of the M5 shield wall at the muon g-2 storage ring room
- obtain residual radiation dose rate estimate for the 907 collimator
- estimate TLM response due to beam loss at the 907 collimator and Q908/Q909 quadrupoles
- provide an estimate of hadron flux in the tunnel air for subsequent determination of air activation potential
- provide estimates of star density in the surrounding tunnel backfill materials and the base soil for determination of surface water and ground water activation
- determine if in-tunnel shielding will be required to mitigate any of the aforementioned concerns

A recent update to the MARS code system [4] features a particle splitting technique at user defined surfaces as a method to obtain statistically significant radiation dose and fluence estimates in deep shielding problems without resorting to the multistage MARS runs. The particle splitting technique has been adopted in this work in two directions of interest, first, in the horizontal plane throughout the shielding berm above the 907 collimator, Q908 and Q909; and second, in vertical planes through the M5 enclosure and the M5 shield wall.

## The M4 Beamline Model

The model of the upstream M4 beamline was developed from the Project 6-10-22 as-built drawings [3], principally, the structural concrete drawings. Site coordinates provided in the as-built drawings were used to establish the precise positioning of the various tunnel sections through the curvature of the tunnel.

The enclosure air volumes are modeled in accordance with the as-built drawings. The nominal concrete density applied to concrete structures is 2.35 g/cc. A GUI image of the entire model at the beam elevation of the 907 collimator is shown on the cover page of this document.

The concrete enclosure structures are typically backfilled with CA-7 to ensure rapid water removal through an underdrain system. The enclosures are modeled with a 3' CA-7 backfill outside of walls and a 1' CA-7 backfill over ceilings. The density of CA-7 used in the model is 1.7 g/cc and is based upon field measurements made on actual material during construction [5]. Disturbed soil, shown in green is modeled with a nominal density of 1.9 g/cc. Glacial till, shown in yellow, is assumed to be undisturbed and is modeled with a nominal density of 2.24 g/cc.

There are two general model regions of interest described in the following subsections: the 907 collimator region and the M5 shield wall region.

### 907 Collimator region model

The 907 collimator region model includes the following features:

- 907 collimator and downstream quads Q908 and Q909
- Upstream exit stairway with tissue equivalent detector at the termination of exit door
- Shielding berm
- Tissue equivalent detector array on surfaces of shielding berm
- TLM detector volumes
- Glacial till volumes near beam loss point
- Tunnel air volumes

Site coordinates for the 907 collimator were provided in Reference 12. Initially, the collimator was placed in the model according to the provided site coordinates as indicated in Figure 1. It was observed in the team center 3D view, also provided in Reference 12, that the collimator was installed closer to the step in the M4 enclosure floor. It was determined from Reference 13 that the collimator was actually installed about 2 meters downstream of the site coordinate position; the model coordinates of the collimator were adjusted accordingly.

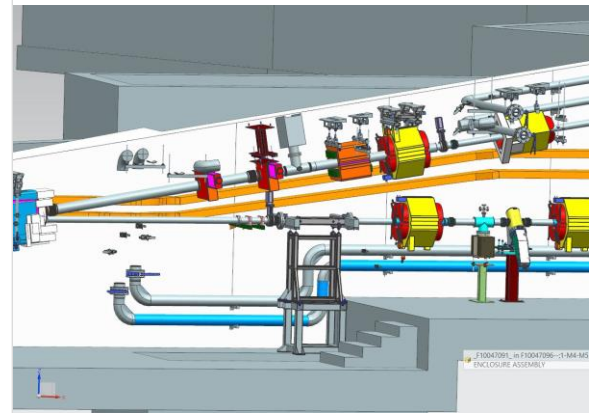
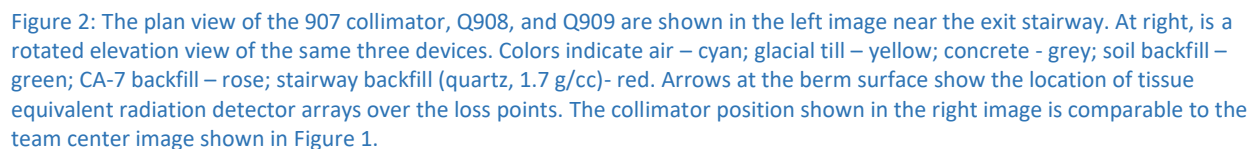


Figure 2 shows a plan view through the horizontal plane of the 907 collimator and the downstream quads Q908 and Q909. These elements are the principal massive elements in which the proton beam [10] halo would be scattered, eventually lost, and which would contribute to all radiological issues identified earlier. The plan of the nearby exit stairway is also shown. Figure 2 includes an elevation view through beam line trajectory showing the tunnel floor step and the shielding berm.



A GUI image of the 907 collimator model plan view is shown in Figure 3. The collimator assembly, less its stand, is modeled based upon drawings provided in Reference 11. The collimator is designed with an adjustable horizontal aperture. The horizontal aperture is set in the MARS model to 1.2 cm at its minimum based upon Reference 12. The 40 inch long collimator jaws are chamfered at each end as shown in Figure 3; the physical length of the collimator jaws at the minimum aperture is 32 inches.

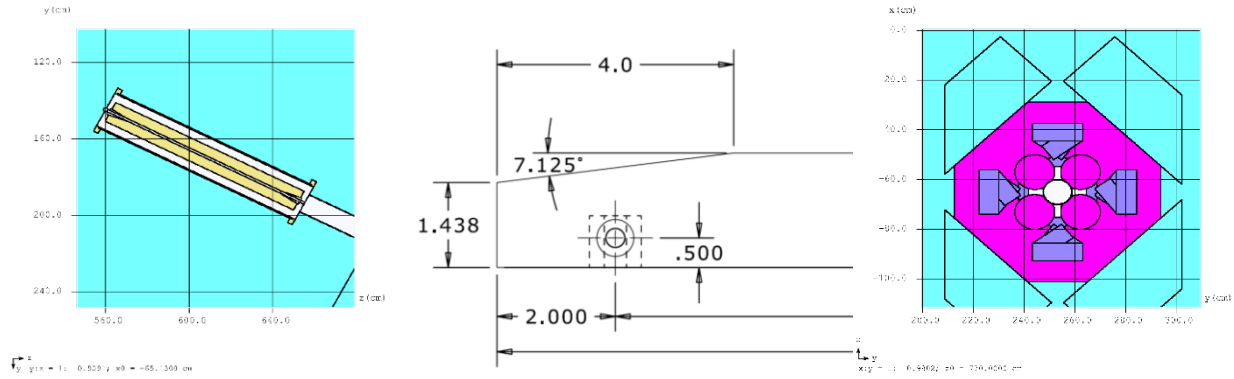


Figure 3: The plan view of the collimator model is shown in the left image. Stainless steel jaws and vacuum vessel are yellow while vacuum space is white. The collimator horizontal aperture is set to 1.2 cm in the model. At center, the leading chamfer detail of a collimator jaw is shown; the trailing edge is similar. The MARS model of the collimator jaws includes this chamfer detail. At right, a typical cross section of the Q908/Q909 quadrupoles is shown.

Figure 4 shows the exit stairway and the associated shielding berm, modeled in accordance with the as-built construction drawings [3]. The second riser of the stairway is located orthogonally from the beam axis of the 907 collimator. A tissue equivalent detector is included in the model at the stairway exit door to estimate the effective radiation dose rate due to normal beam loss on the collimator.

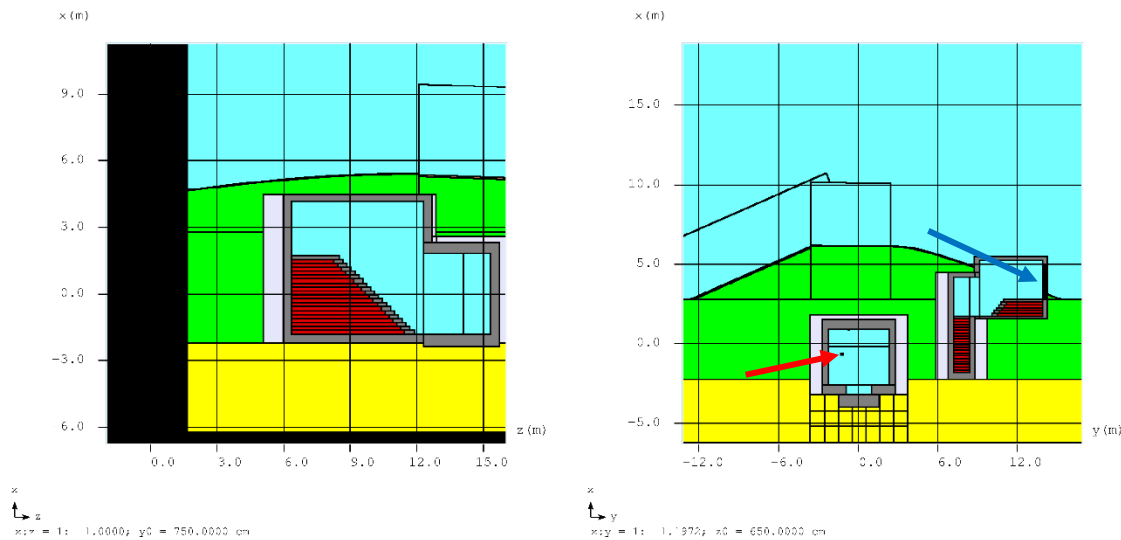


Figure 4: A midline elevation view of the first riser of the exit stairway is shown at left and of the second riser is shown at right. The collimator position is indicated by the red arrow. A tissue equivalent mass positioned at the exit stairway door is indicated by the blue arrow.

One of the difficulties in preparing this model is due to the non-linear arrangement of the various tunnel sections. The normal Z axis of the model is parallel with the M5 enclosure straight section while the M4

tunnel sections are not. At this time [14], xyz histograms can only be aligned with the MARS xyz axes. Histograms for prompt effective dose rate due to normal beam loss on the 907 collimator and Q908/Q909 quadrupoles are provided at the Z = 150 cm and 560 cm positions shown in Figure 5; at the z=655 cm and 750 cm positions in Figure 6; and at the z = 790 cm and 970 cm positions in Figure 7.

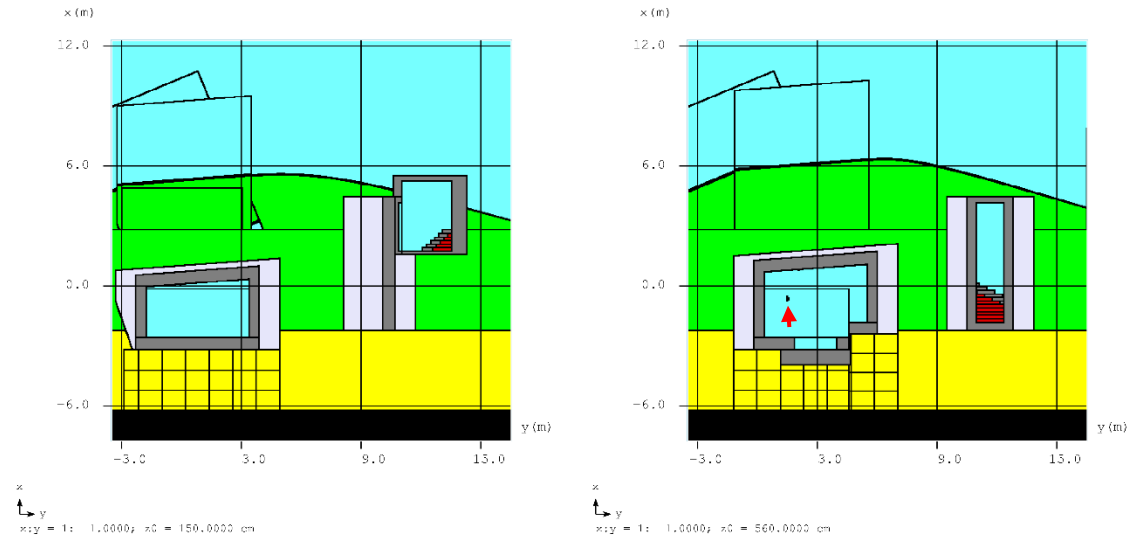


Figure 5: Elevation view of the M4 beam line and exit stairway riser 2 at z = 150 cm (left) and exit stairway riser 1 at z = 560 cm (right). The lift platform pit is also visible in the right image. Tissue equivalent detectors are indicated by heavy black lines on the surface of the shielding berm. The red arrow in the right image indicates the upstream end of the 907 collimator.

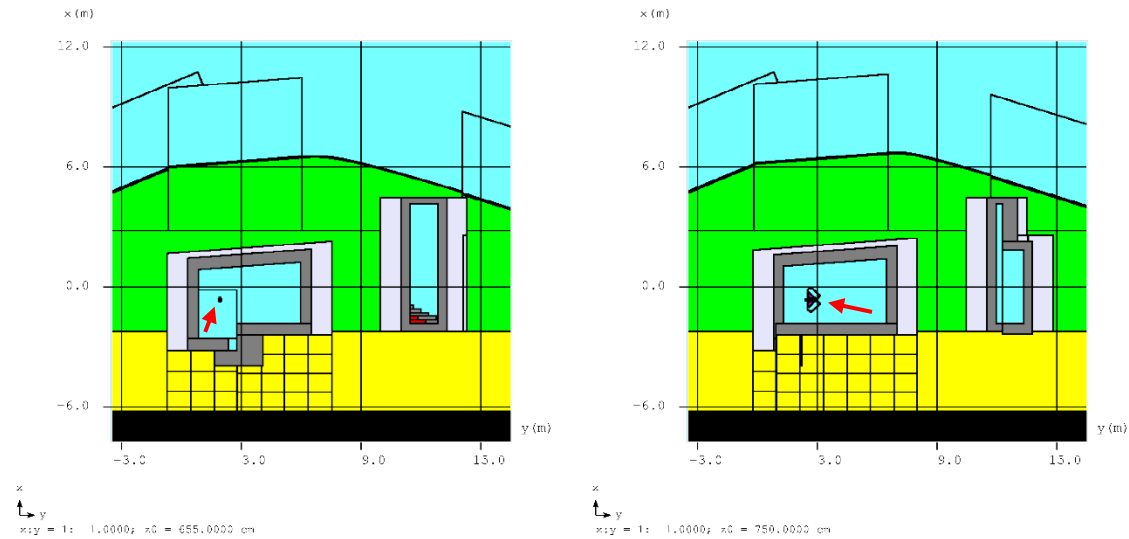


Figure 6: Elevation view of the M4 beam line and exit stairway riser 1 at z = 655 cm (left) is shown; the red arrow indicates the downstream end of the 907 collimator. At right, the upstream end of the Q908 quadrupole position is shown relative to exit stairway riser 1 at z = 750 cm (right). Tissue equivalent detectors are indicated by heavy black lines on the surface of the shielding berm.

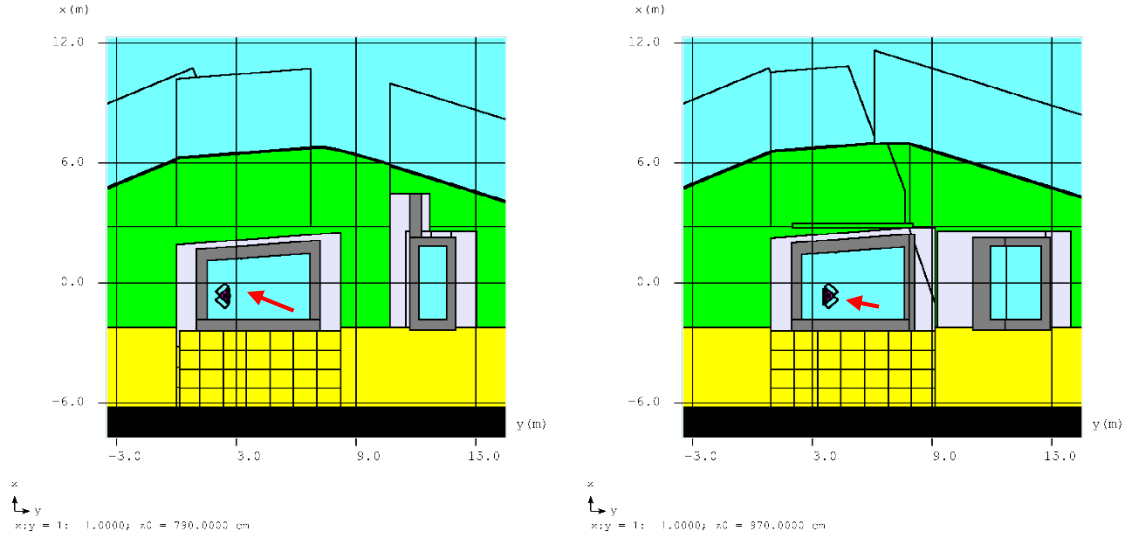


Figure 7: Elevation view of the M4 beam line and exit stairway riser 2 at  $z = 790$  cm is shown at left; the red arrow indicates the downstream end of Q908. At right, the upstream end of Q909 is indicated by the red arrow and its position relative to the exit stairway entrance at  $z = 970$  cm. Tissue equivalent detectors are indicated by heavy black lines on the surface of the shielding berm.

To estimate the TLMs response due to beam loss on the 907 collimator and Q908/Q909, a 61.6 meter long TLM detector has been modeled as shown in Figure 8. The TLM detector model [7], is positioned near the ceiling at the centerline of each tunnel section as shown in Figure 9 and Figure 10. The TLM cable model consists of 8 major sections. The first 4 sections are subdivided into approximate 1 meter lengths while the last four sections are continuous lengths. The purpose of the subdivisions is to estimate the regions of peak response. A summary of the detector cable lengths is shown in Table 1.

Detector	Total length (m)	Number of subdivisions	Length per subdivision (m)
1	12.4	12	1.03
2	3.38	3	1.12
3	7.18	7	1.05
4	5.56	6	0.93
5	8.77	1	8.77
6	6.8	1	6.8
7	6.31	1	6.31
8	11.22	1	11.22

Table 1: A breakdown of the TLM detector cable sections is given in the table.



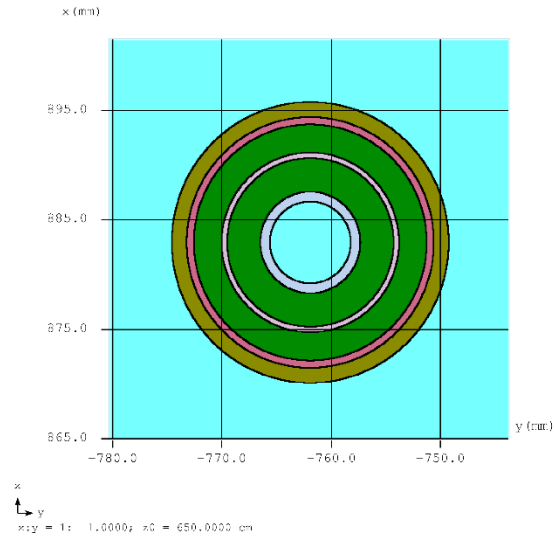


Figure 8: A cross section of TLM detector cable is shown in the image; detector material starting from the center circle and progressing radially outward are: air, copper, detector gas, polyethylene standoff insulator, detector gas, copper, and polyethylene jacket.

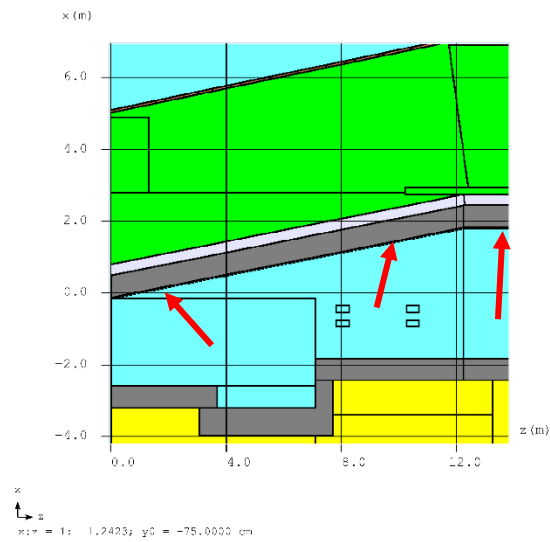


Figure 9: The TLM location in the first two sections of tunnel are indicated in the image (red arrows).

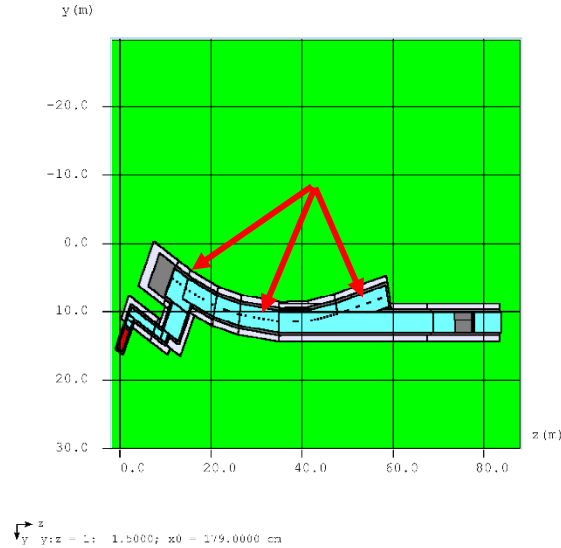


Figure 10: TLM sections beyond the first sloped ceiling tunnel section are shown in this image (red arrows). The TLMs are placed near the tunnel ceiling ( $x = 179$  cm) at the centerline of each section.

### M5 shield wall region

The M5 tunnel has been modeled in some detail to estimate radiation effective dose rates downstream of the M5 shield wall, adjacent to the g-2 storage ring room. The tunnel section is modeled based upon as-built drawings [3]. The M5 shield wall is modeled as shown in Figure 14 and based upon information provided in Reference 15. Figure 11 shows MARS GUI images of the elevation cross sections through the M5 shield wall and the tissue equivalent detector modeled just downstream of the shield wall. Figure 12 shows longitudinal elevation views through the M5 shield wall and includes some details of the cable penetrations which are routed between the upstream and downstream sides of the shield wall. Figure 13 shows additional penetrations through the shield wall and a plan view of the shield wall footprint. Since the radiation shower originates upstream at the 907 collimator, the shielding berm above the M5 line and downstream sections of the M4 line have not been modeled.

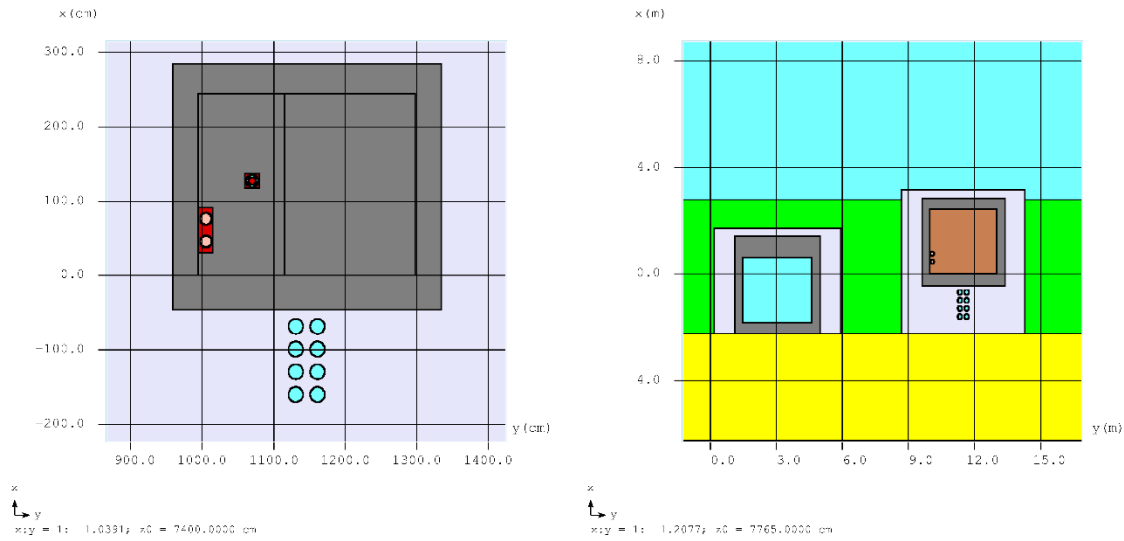


Figure 11: The left image shows an elevation view of the M5 tunnel which includes the beam pipe and water header penetrations and cable penetrations which pass longitudinally beneath the upper floor of the M5 tunnel. At right, an elevation view of the M4 (left) and M5 tunnels is shown through the plane of the modeled tissue equivalent detector just downstream of the M5 shield wall. The shield berm above this section of tunnel is absent since it has no bearing on the radiological issues under study in this report.

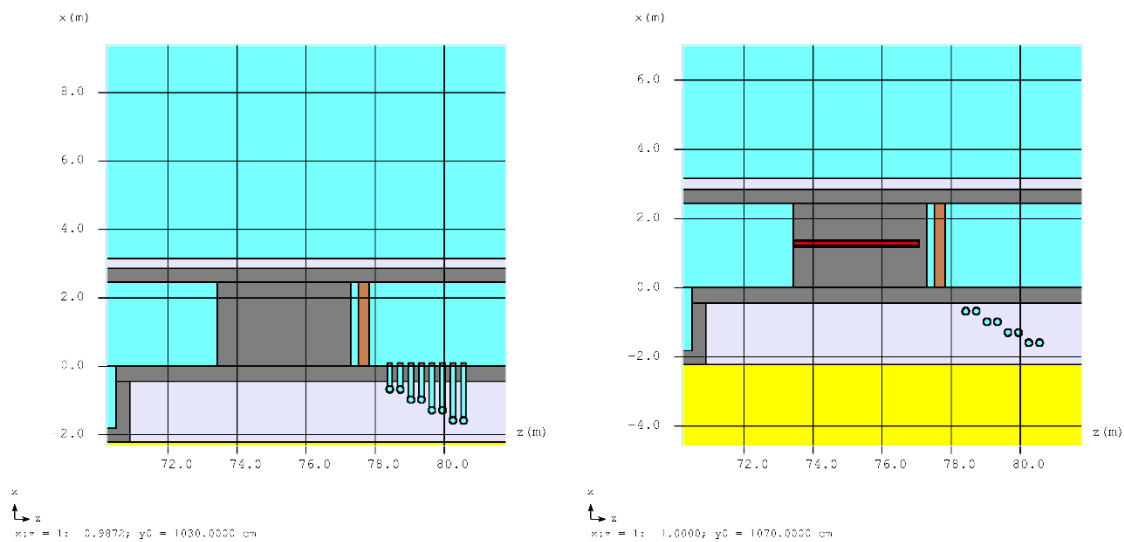


Figure 12: At left, a partial elevation view of the M5 tunnel is shown through the section where the cable penetrations emerge from the floor downstream of the shield wall. A tissue equivalent mass is located at the exit of each penetration. At right, a similar elevation view is shown through the section in which the beam pipe passes through the shield wall. The brown volume is the single volume, tissue equivalent detector. The shielding berm above the M5 tunnel has not been modeled.

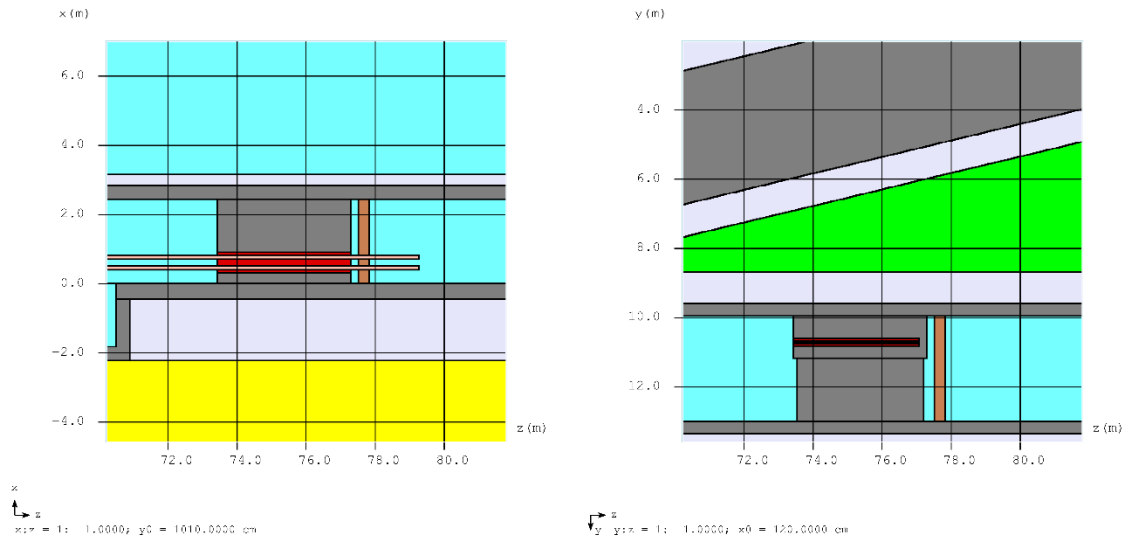


Figure 13: At left, a partial elevation view of the M5 tunnel is shown through the section where the water headers pass through the M5 shield wall. At right, a plan view of the M5 shield wall is shown through the elevation at which the beam pipe passes. The beam left portion of the wall (upper gray rectangle) is constructed of hand-stacked concrete blocks with a density of 2.13 g/cc. The beam right portion of the wall (lower gray rectangle) is composed primarily of concrete blocks modeled with a density of 2.35 g/cc.

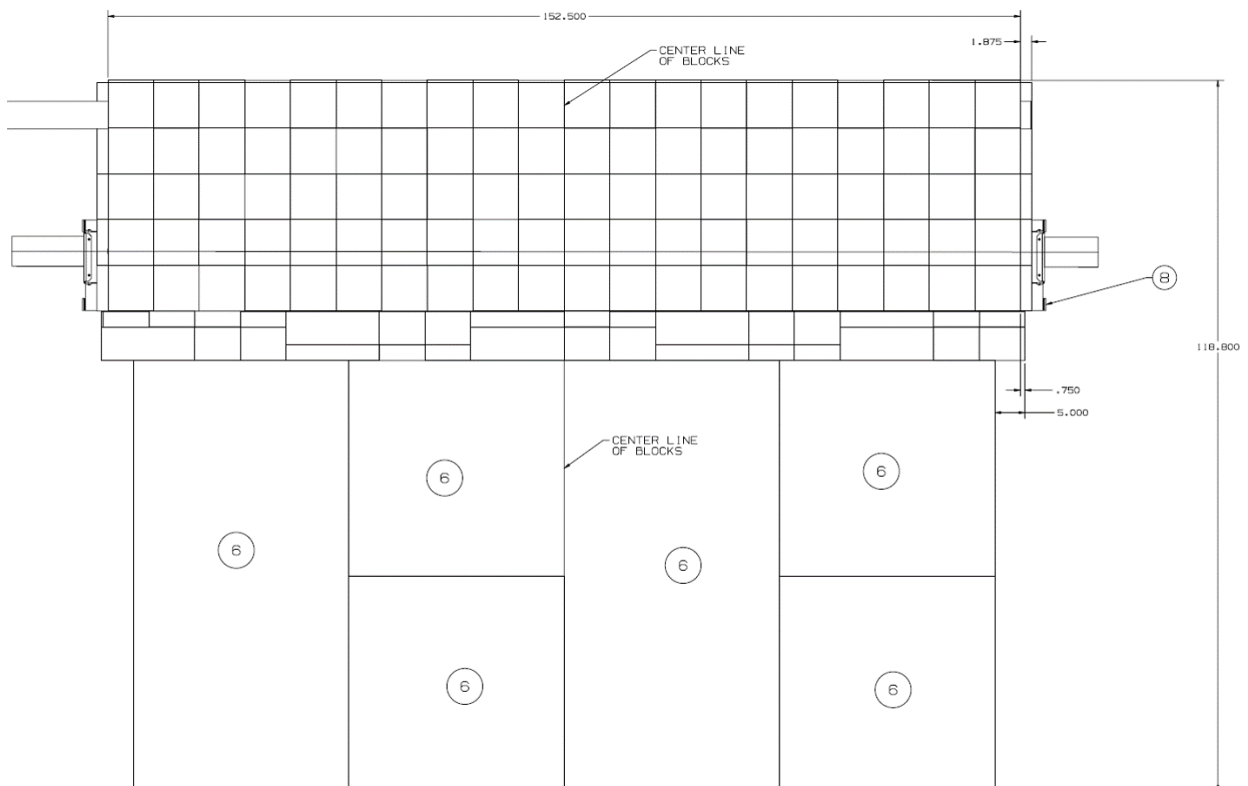


Figure 14: Stacking plan view of the M5 shield wall provided from Reference 15. The hand stacked block density is modeled at 2.13 g/cc while the larger concrete blocks are modeled with a density of 2.35 g/cc.

## Particle splitting

A relatively new technique [4] is used in this simulation work to address the deep penetration, thick shielding situations presented by the problem. The particle splitting technique is designed as a single-run replacement to a multi-step, intermediate source approach. The rationale for using this technique is to eliminate the creation and subsequent reading of huge source files which had become a bottleneck in distributed computing environment.

To implement particle splitting, arbitrary particle crossing surfaces were established in a user input file (BRANCH.INP). Shower propagation through the model was set up for the two thick shields interest: 1. the shielding berm above the 907 collimator and Q908/Q909 and, 2. the M5 shield wall upstream of the muon g-2 storage ring room. For the 907 collimator region, 5 horizontal planes set at 1 meter intervals were used as shown in Figure 15; particle splitting was applied to neutrons and high energy photons. Due to the ~70-meter distance through the M4/M5 tunnel from the loss point at the 907 collimator to the upstream face of the M5 shield wall, two vertical planes orthogonal to the MARS z axis were added to amplify the source. Upon reaching the M5 shield wall, five vertical planes were positioned across the M5 shield wall, to achieve statistically meaningful results at the tissue equivalent detectors located downstream of the M5 shield wall. Since the M5 shield wall is off the central axis of the proton beam at the collimator, only neutron particle splitting was applied for these surfaces.

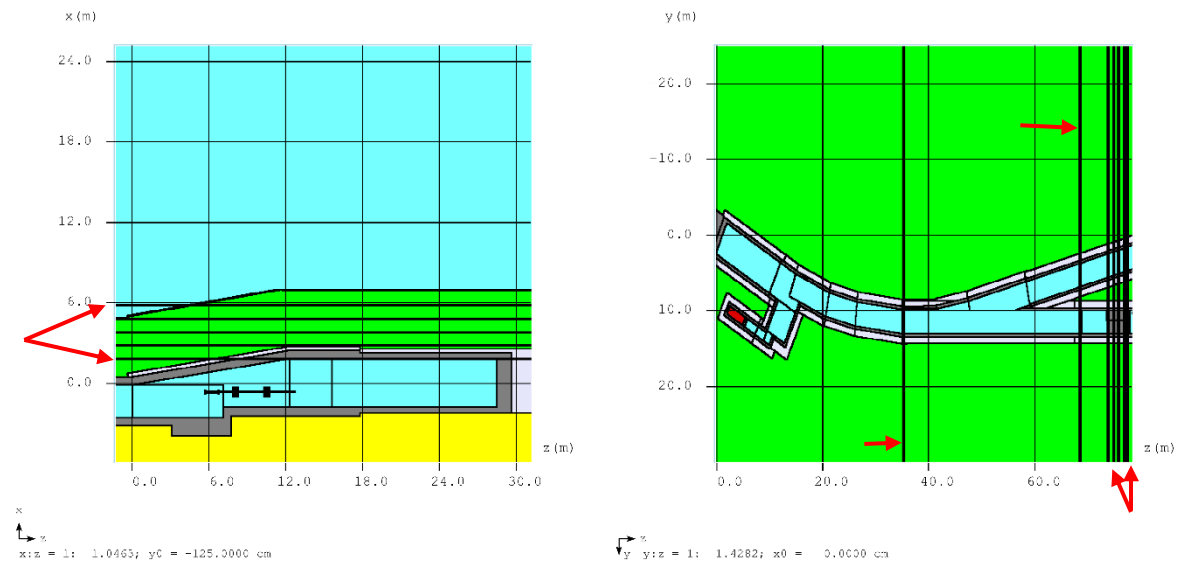


Figure 15: At left, 5 horizontal crossing surfaces were placed in the model for particle splitting including neutrons and photons. At right, 7 vertical crossing surfaces were placed for neutron particle splitting.

With the particle splitting parameters set, the number of events and number of jobs were set to develop dose estimates in radiation sensitive volumes with sufficiently low variance. The effective dose rate results provided in subsequent sections are the result of the choices made in the branching parameters. The total CPU time required to achieve the normal condition result for each run was approximately 5 years.

## MARS Simulation

A beam source file consisting of 452,931 protons transported from the extraction system at MI30 was provided in Reference 10. The beam initial position is arbitrarily located at US end of collimator. The source file provides the proton energy, horizontal and vertical position with respect to the central axis of the collimator, and the angular kick in the horizontal and vertical planes. The proton beam energy ranges from the nominal 8 GeV beam energy to 7.929 GeV. The source file was cycled for 3 passes for each of the 2,000 jobs submitted. Only about 1530 jobs of those submitted for each attempt was completed successfully. Several subsequent sets of jobs were supplied with a new random number seed; selected runs were combined to reduce results variances. All histogram results shown below are in units of mSv/hr normalized to a beam intensity of  $6.25 \times 10^{12}$  protons/second; only about 0.28% of the beam is lost on the collimator. The remaining beam is stopped in a black hole volume positioned at the end of the vacuum tube and does not contribute to indicated radiation dose rates.

## Simulation results

Results from the MARS simulation includes histograms, tissue equivalent detectors, air activation, surface water activation, groundwater activation, TLM detector results, and residual activation results. These are covered individually in the following sections.

### Prompt Effective Dose Rate Histograms

Figure 16 through Figure 25 shows effective dose rate results for various shield locations described previously. All color histogram results are displayed in units of mSv/hr. Where peak dose rates are reported (units of mrem/hr or urem/hr), they were arrived at by active inspection of the MARS GUI image.

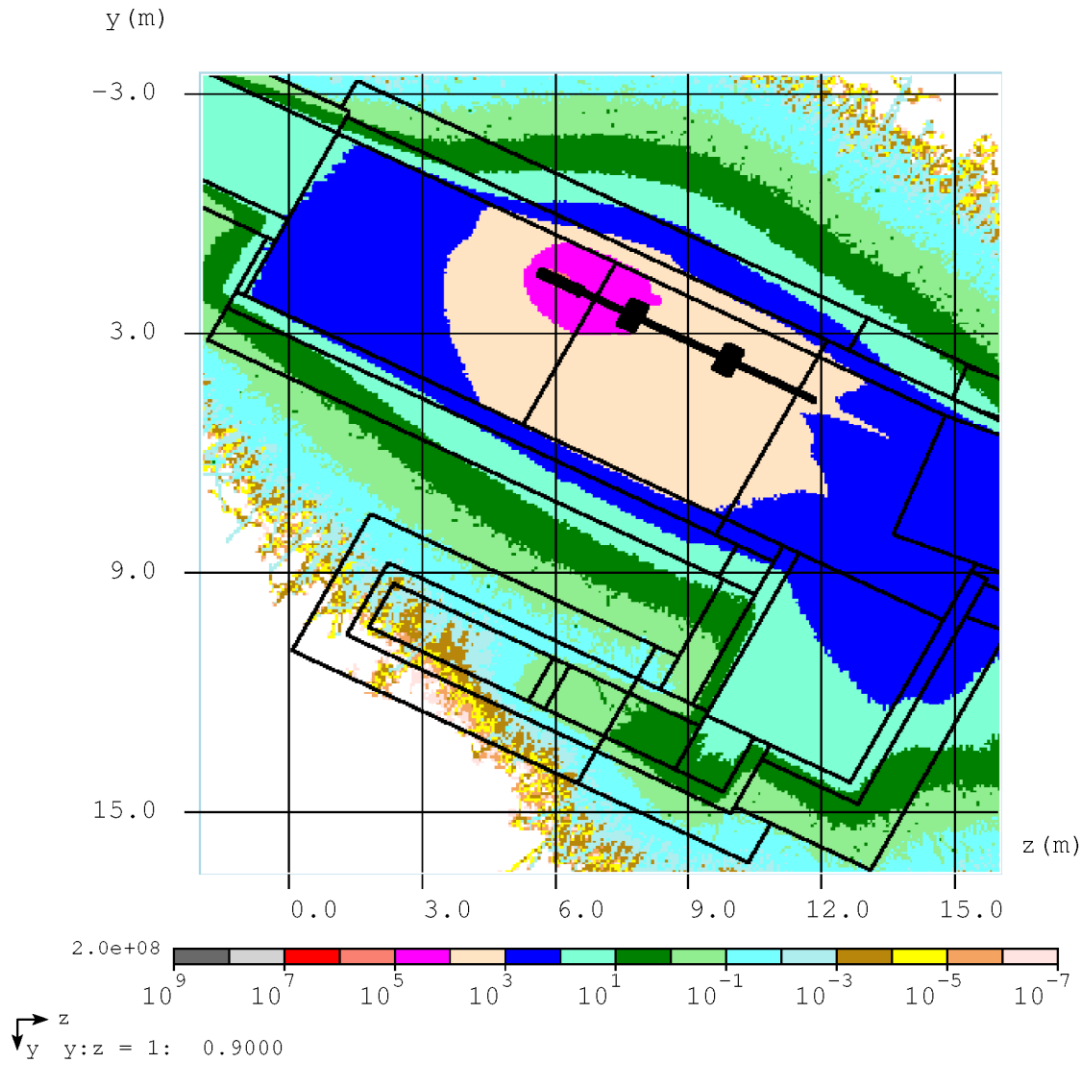


Figure 16: This prompt dose rate histogram shows a plan view of the collimator region at the beam elevation  $x = -65.13$ . The beam is being lost in the collimator and the shower extends to and is suppressed by quadrupole Q908.

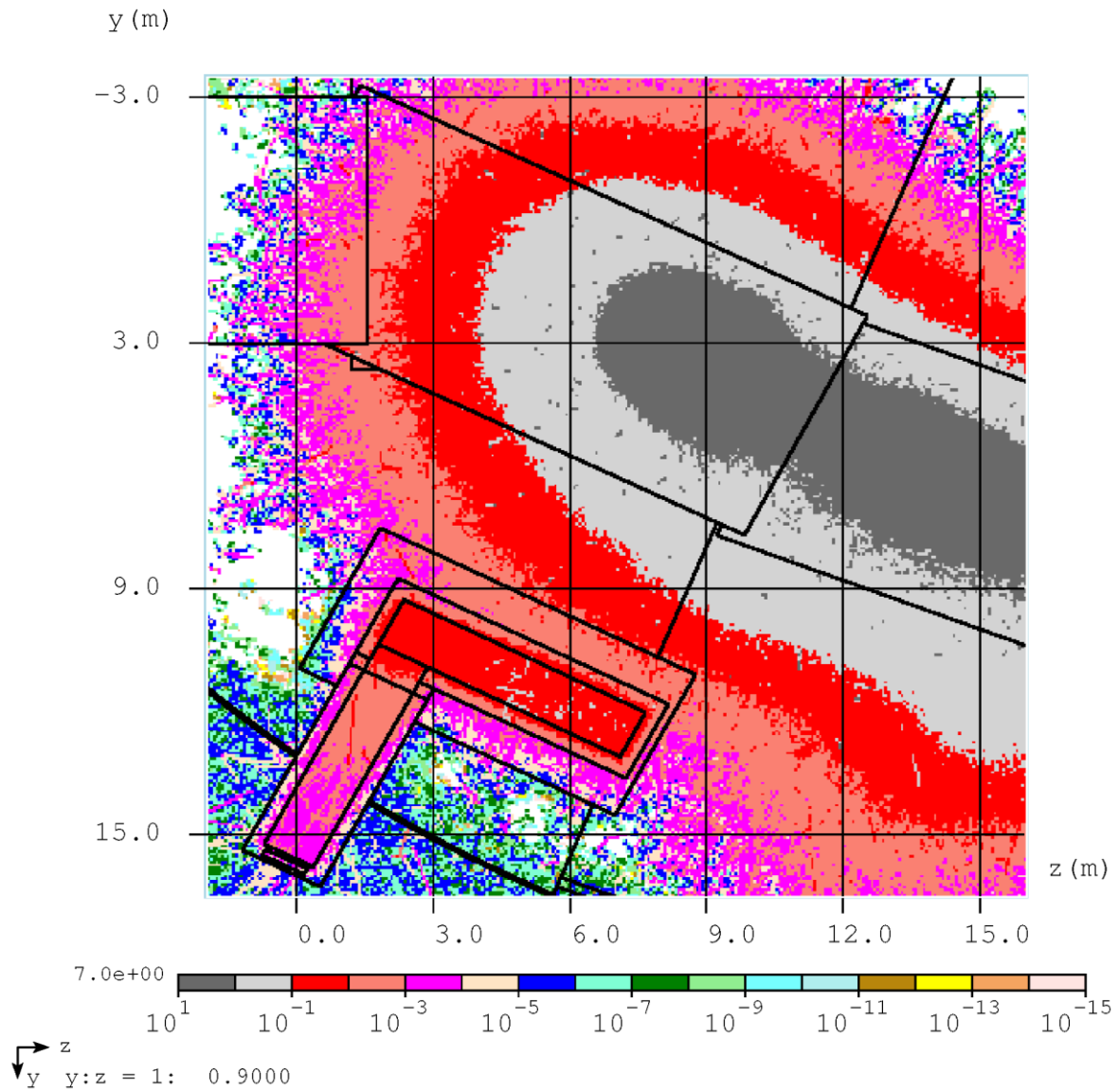


Figure 17: Prompt effective dose rates here are at  $x = 390$  cm, the elevation midpoint through the nearby exit stair doorway.



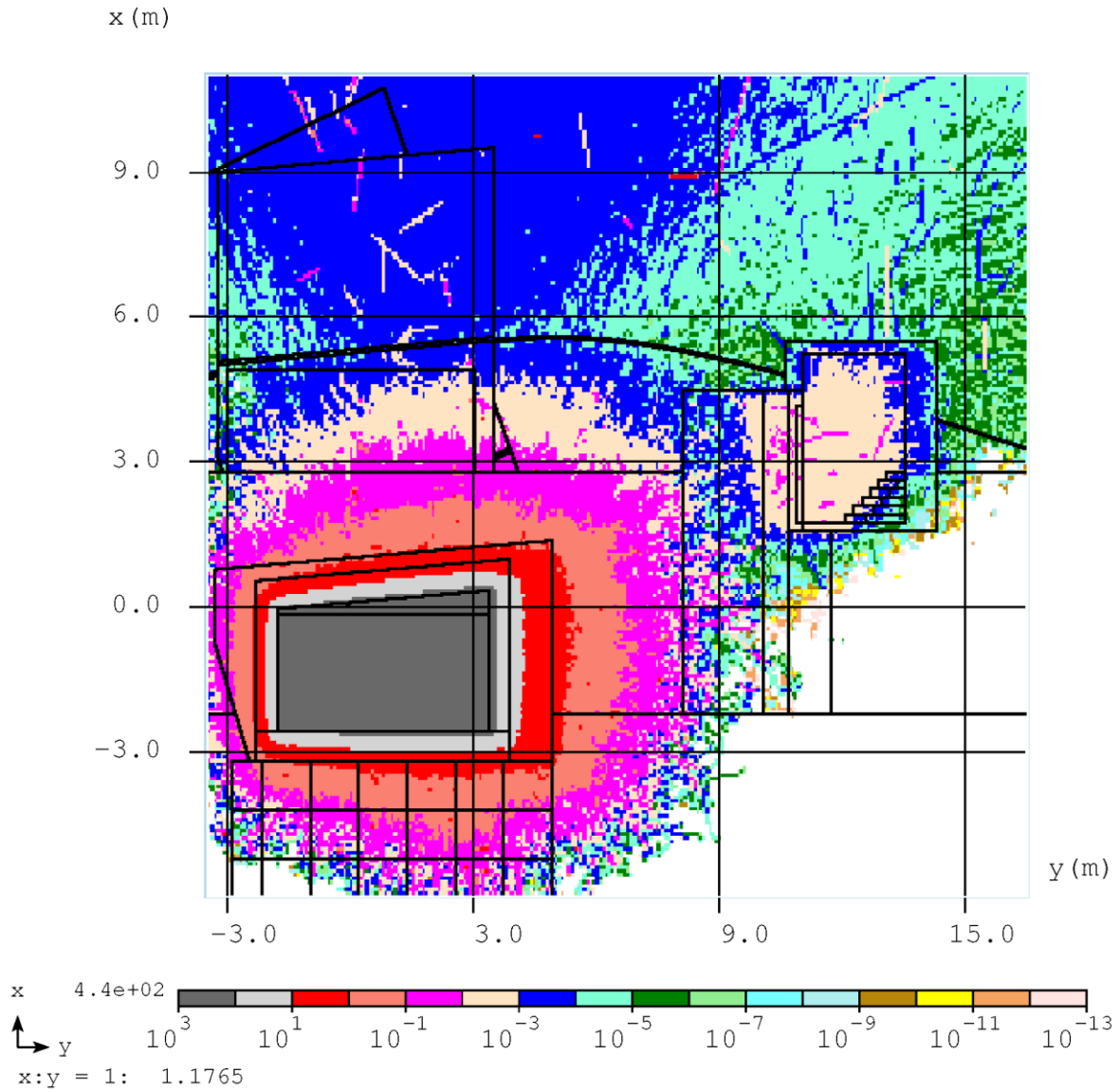


Figure 18: This prompt dose rate histogram shows a skewed view of the berm cross section at  $z = 150$  cm. The cross section passes about 4 meters upstream of the 907 collimator and through the exit stair doorway. The peak prompt dose rate at the berm surface is approximately 25 urem/hr.

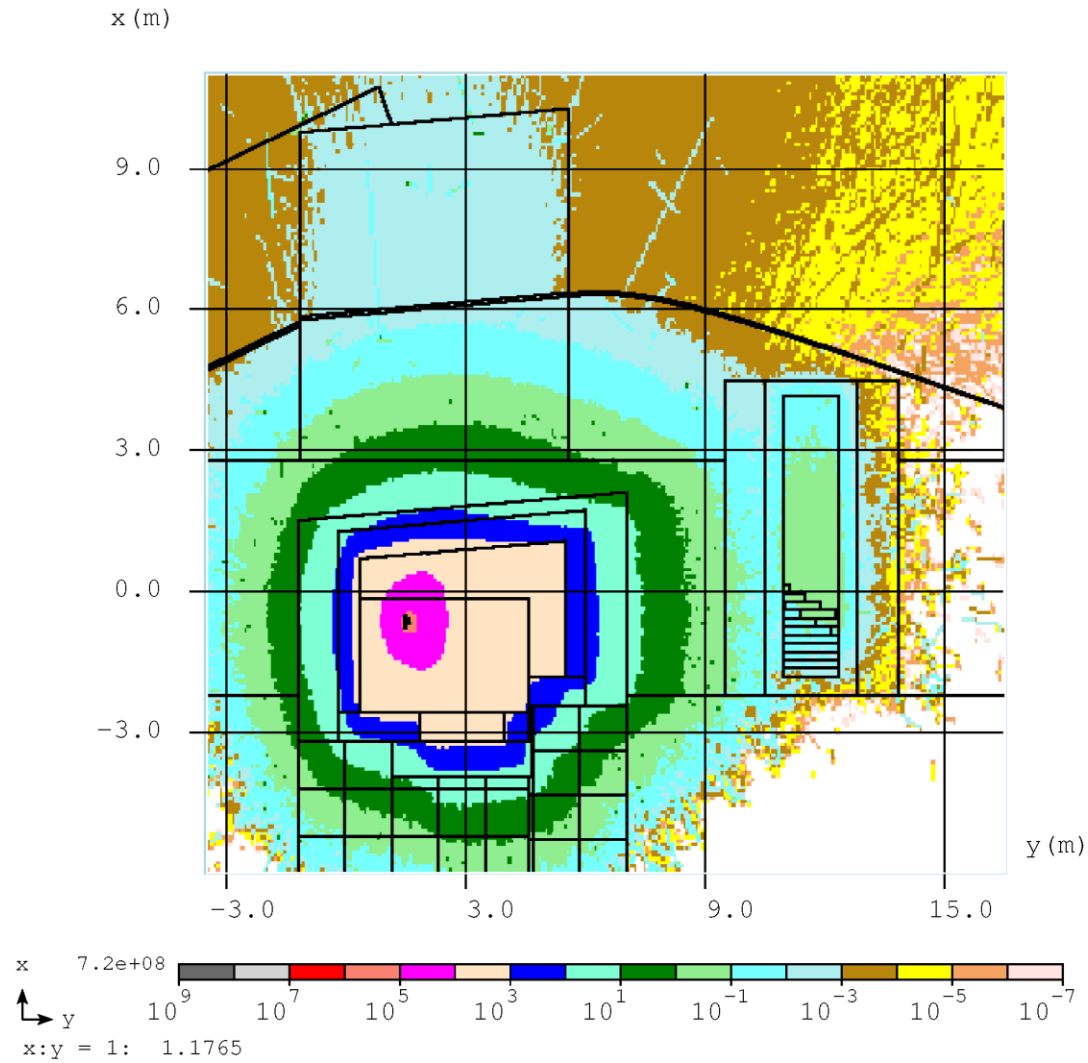


Figure 19: This prompt dose rate histogram shows a skewed view of the berm cross section at  $z = 560$  cm. The cross section passes the upstream end of the 907 collimator and through the first stairway riser. The peak prompt dose rate at the berm surface is approximately 0.3 mrem/hr.

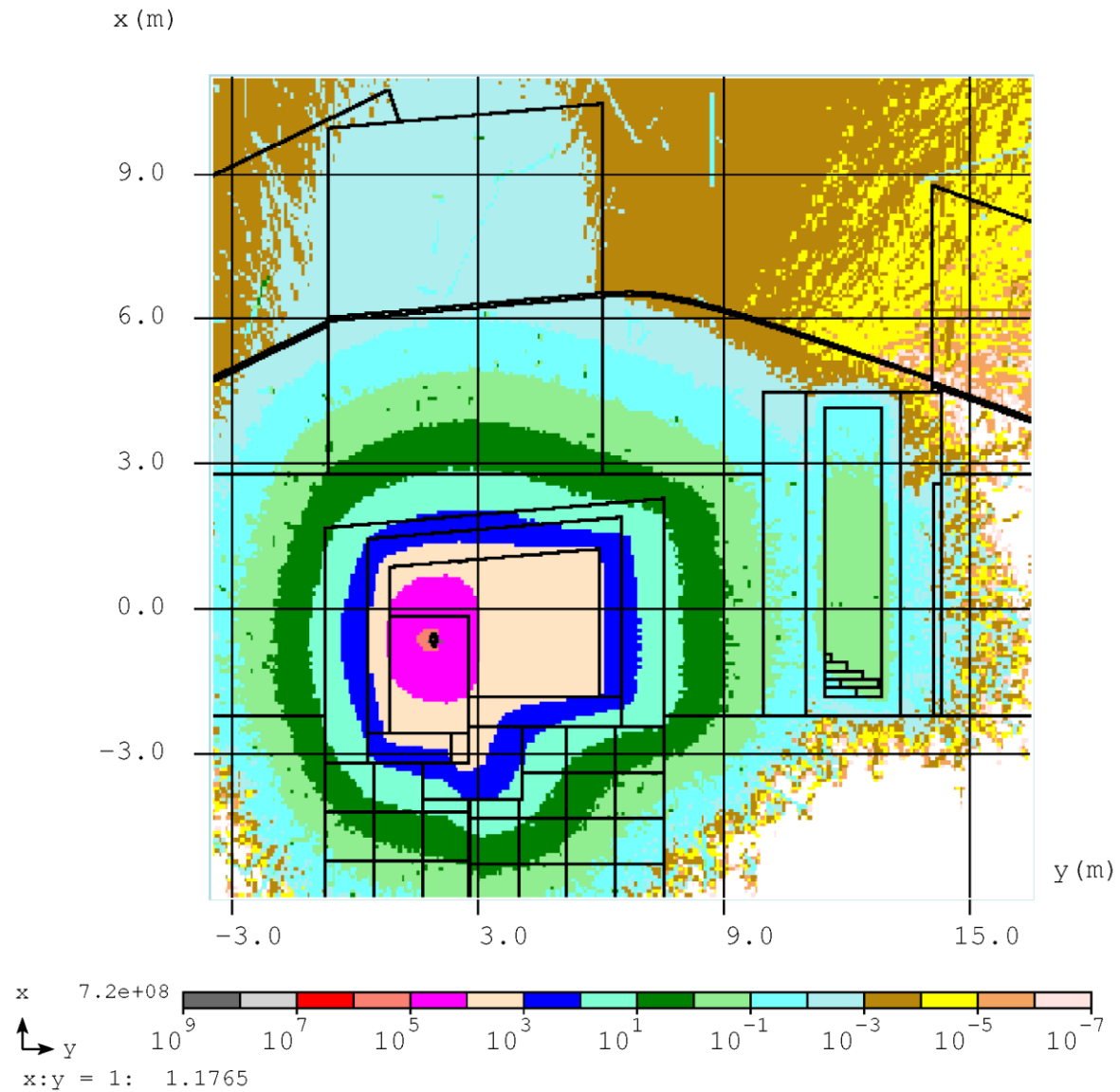


Figure 20: This prompt dose rate histogram shows a skewed view of the berm cross section at  $z = 655$  cm. The cross section passes through the downstream end of the 907 collimator and through the first stairway riser. The peak prompt dose rate at the berm surface is approximately 0.4 mrem/hr.

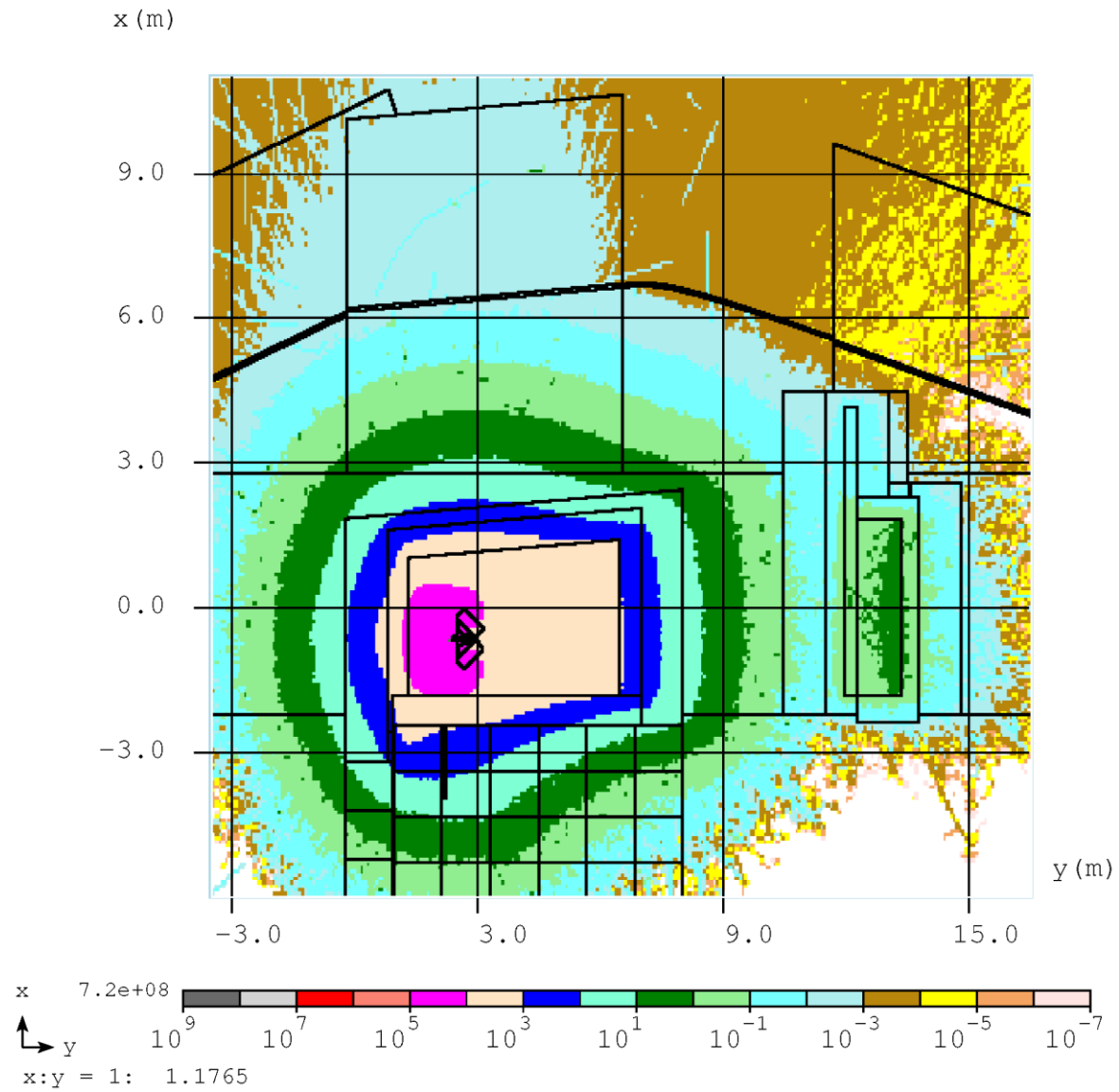


Figure 21: This prompt dose rate histogram shows a skewed view of the berm cross section at  $z = 750$  cm. The cross section passes through the upstream end of the Q908 quadrupole and through the exit stair tunnel alcove. The peak prompt dose rate at the berm surface is approximately 0.4 mrem/hr.

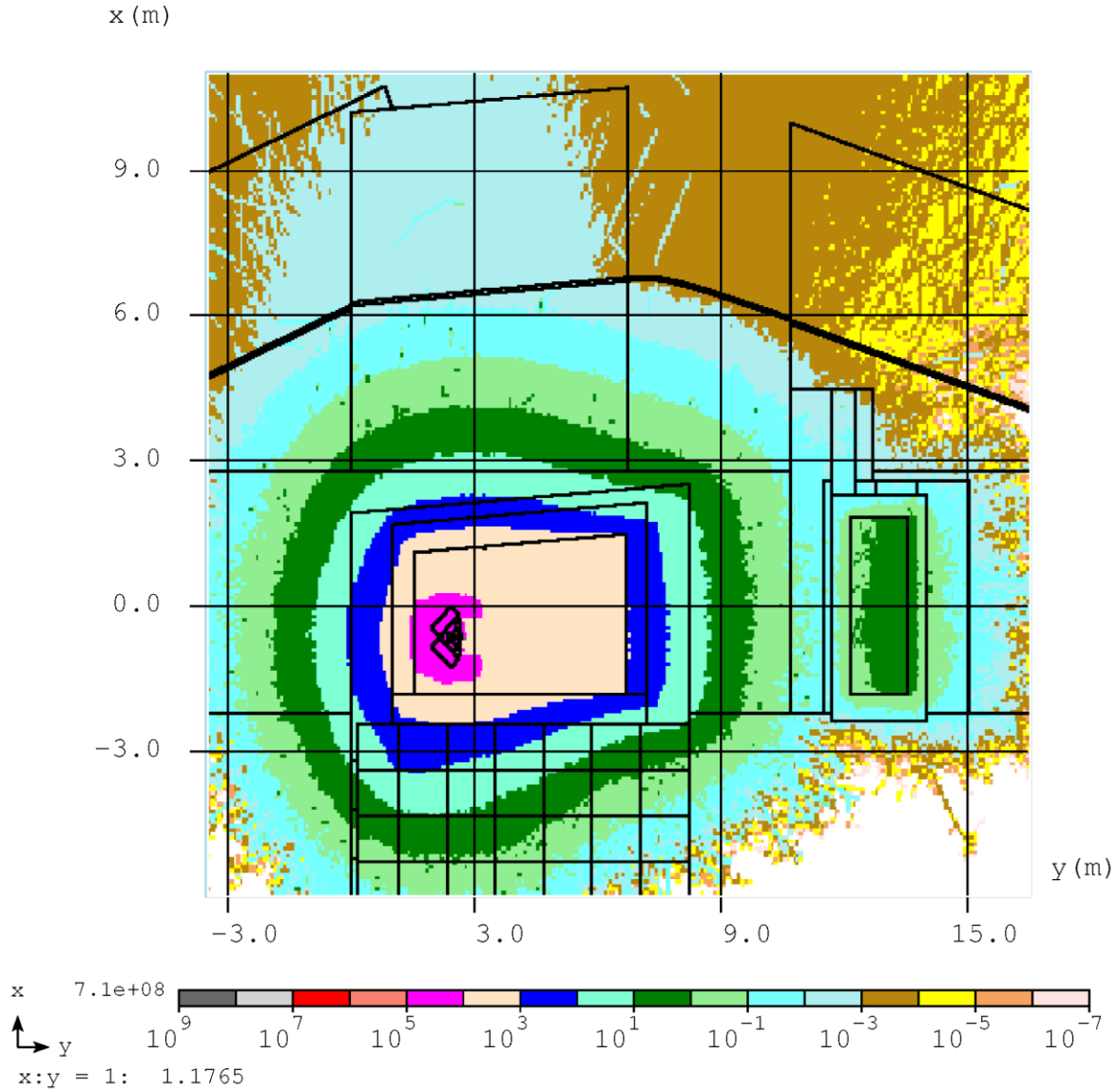


Figure 22: This prompt dose rate histogram shows a skewed view of the berm cross section at  $z = 790$  cm. The cross section passes through the downstream end of the Q908 quadrupole and through the exit stair tunnel alcove. The peak prompt dose rate at the berm surface is approximately 0.4 mrem/hr.

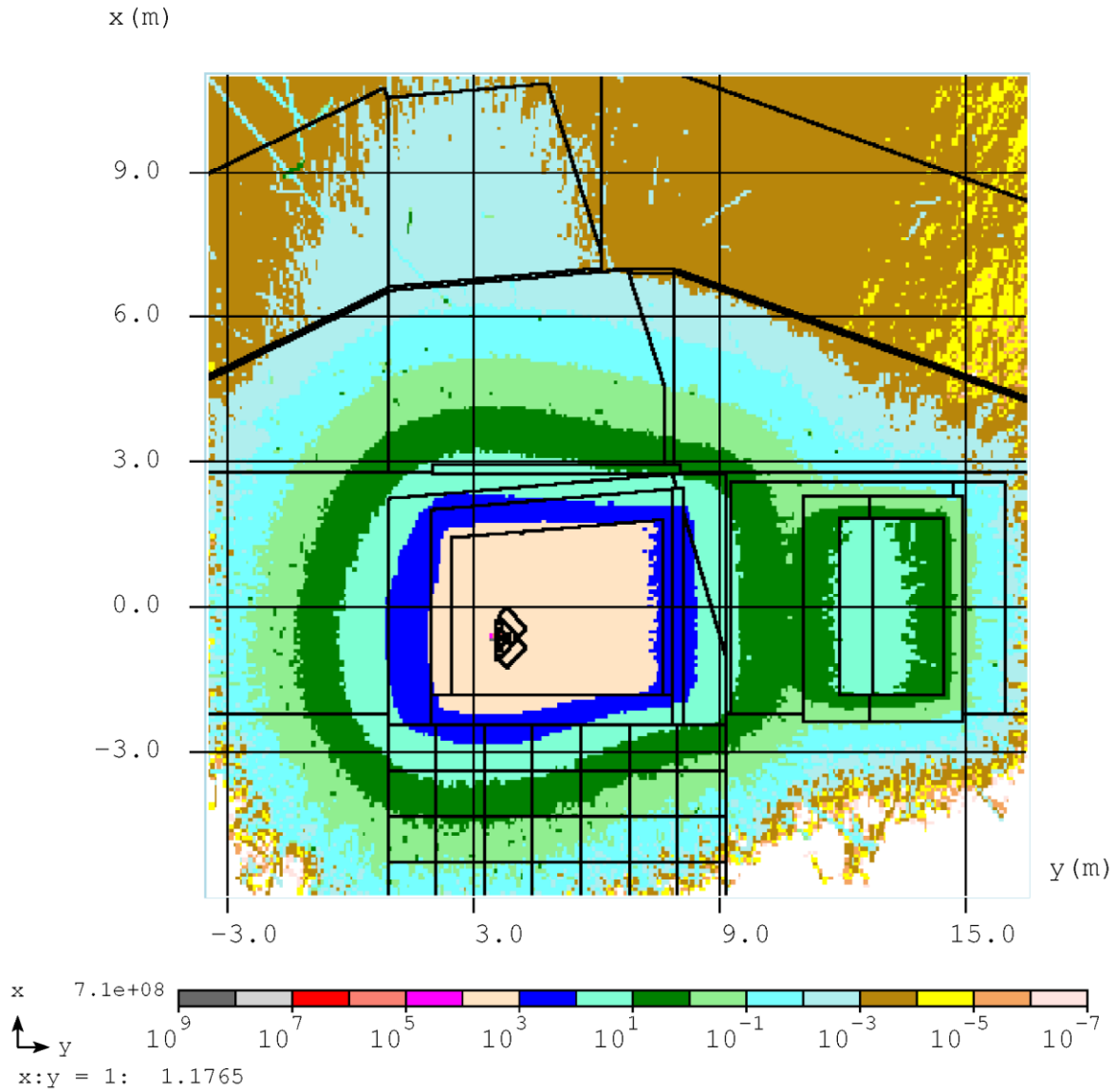


Figure 23: This prompt dose rate histogram shows a skewed view of the berm cross section at  $z = 970$  cm. The cross section passes through the upstream end of the Q909 quadrupole and through the exit stair tunnel alcove. The peak prompt dose rate at the berm surface is approximately 0.2 mrem/hr.

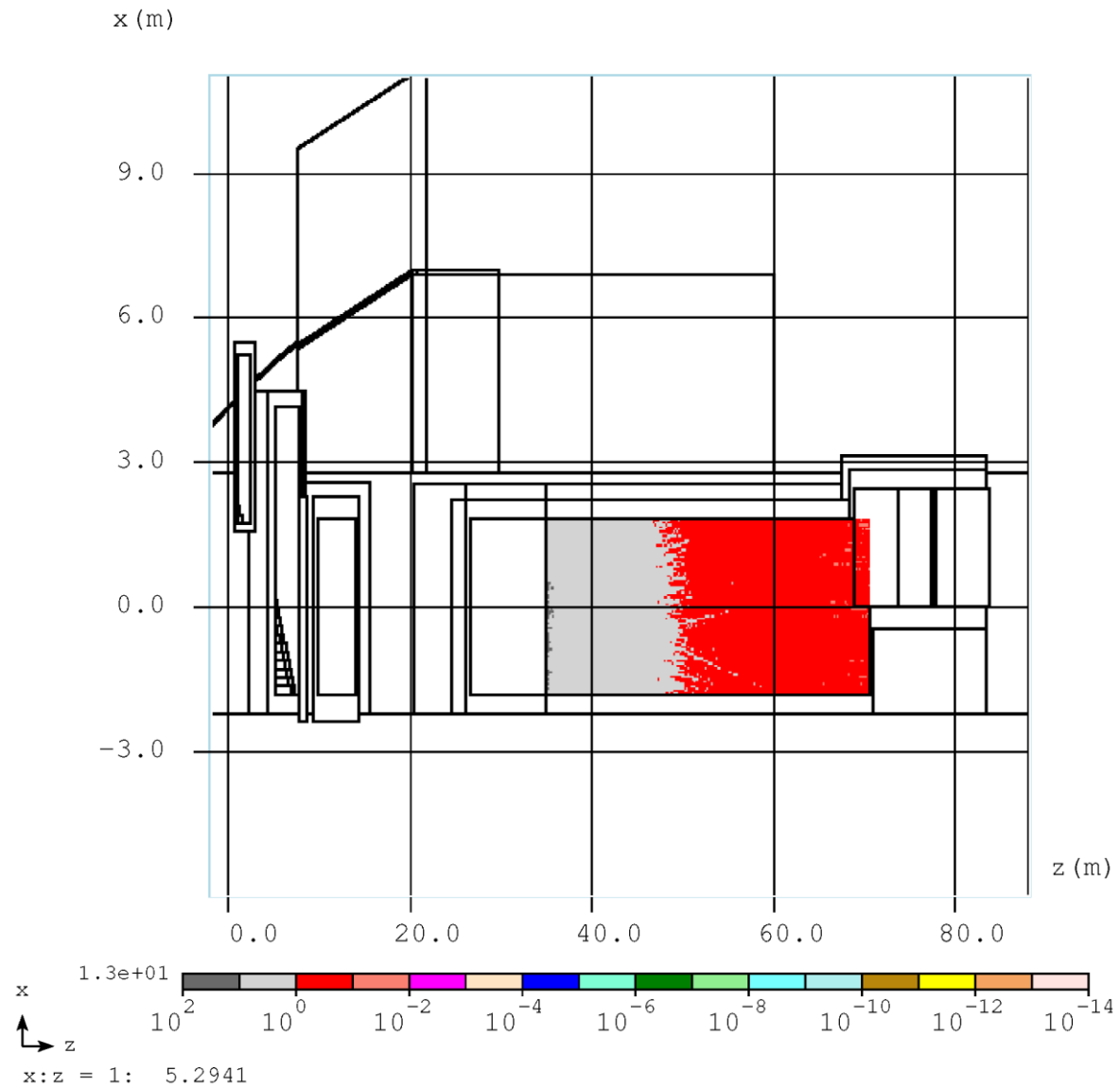


Figure 24: This prompt dose rate histogram shows a longitudinal elevation view at the M5 tunnel centerline. The prompt dose rate at the step is approximately 20 mrem/hr due to normal losses at the 907 collimator.

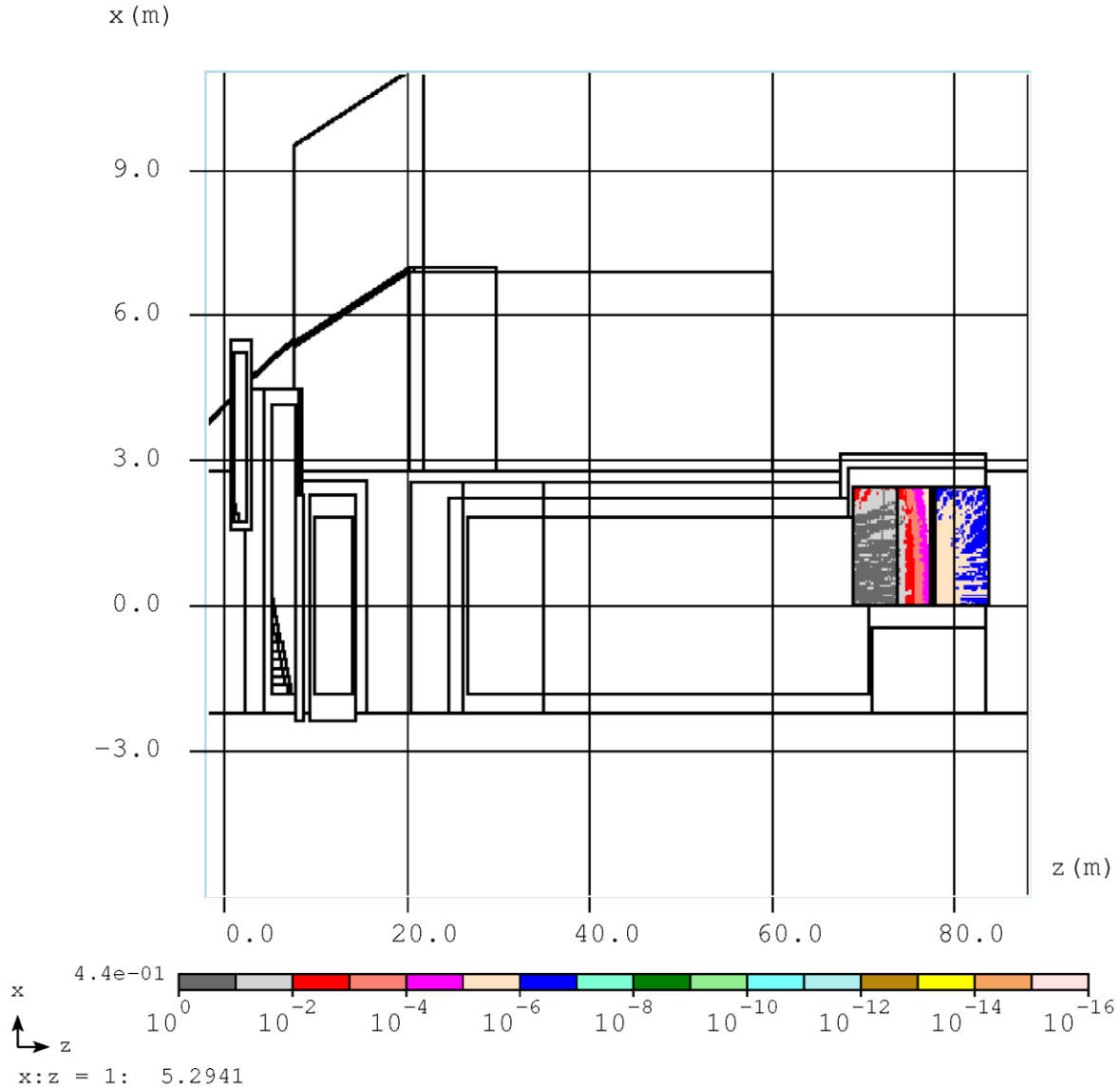


Figure 25: This prompt dose rate histogram shows a longitudinal elevation view at upper the M5 tunnel centerline. The prompt dose rate at the tissue equivalent detector downstream of the M5 shield wall is  $< 50$   $\mu\text{rem/hr}$  due to normal losses at the 907 collimator.

### Tissue Equivalent Detectors

Results for tissue equivalent detectors are reported in this section. These detector results are taken from the MTUPLE.EXG output files and are provided in units of  $\text{mSv/proton}$  along with a statistical error. The results for the exit stairway, M5 shield wall detector, and the M5 shield wall penetrations are summarized in Table 2 along with the reported error. It is advised [1] that errors less than 20% are required for result to have physical validity. Results obtained which have an error of  $>20\%$  have been included (grey highlight) but should not be relied upon. The results for similar nearby detectors could be considered representative in those cases.



volume	urem/hr	%error
Exit stair doorway	32.09	12.7%
M5 shield wall	0.35	13.9%
M5 shield wall Pen 1	0.08	36.1%
M5 shield wall Pen 2	0.07	58.6%
M5 shield wall Pen 3	0.15	46.2%
M5 shield wall Pen 4	0.14	73.7%
M5 shield wall Pen 5	0.19	50.9%
M5 shield wall Pen 6	0.08	37.3%
M5 shield wall Pen 7	0.11	29.7%
M5 shield wall Pen 8	0.56	68.7%

Table 2: Individual tissue equivalent radiation detectors placed at some positions of interest are reported in the table. Results with an error exceeding 20% are not considered to have physical validity; they are reported here for completeness. The effective dose rate reported for radiation leakage through the M5 shield wall detector volume is both physically valid and is the dominant source in the space adjacent to the mu2e storage ring room.

Additional sets of tissue equivalent detectors were used on the surface of the berm as shown in Figure 26. Values reported in the MARS output file are shown in Figure 27. Blank cells indicate that reported variance was >20%. The result for detector array 1 is in reasonable agreement with results shown in Figure 16 through Figure 23.

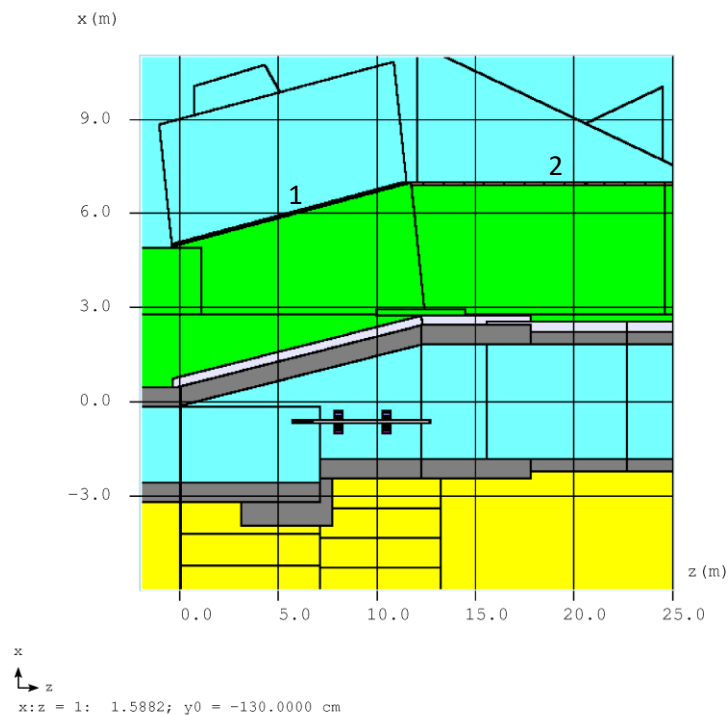


Figure 26: A set of tissue equivalent detectors was placed on the berm surfaces. The sloping berm surface indicated by “1” is a 6 x 12 array of detectors. The surface indicated by “2” is a 6 x 13 array of detectors. The detector areas are approximately 1 m x 1 m.

brm1det	mrem/hr											
	0.01						0.35	0.29				
	0.01						0.44					0.15
					0.28					0.30		
								0.47				0.16
					0.19				0.25			0.13
		0.01			0.11		0.15	0.16		0.12		0.09
brm2det												
0.00			0.01	0.01	0.01				0.00	0.00	0.00	0.00
0.01	0.01	0.02	0.04	0.04	0.03	0.03	0.02	0.01		0.01	0.00	0.00
		0.01	0.05	0.05	0.05		0.04		0.02	0.01	0.01	0.00
	0.01	0.01	0.03	0.05	0.05	0.05	0.05	0.03		0.01	0.01	0.00
0.01	0.01	0.01	0.02	0.04	0.04	0.04	0.04		0.02		0.01	
0.01	0.01	0.02	0.02	0.02	0.02	0.02	0.02	0.02			0.00	0.00

Figure 27: The effective dose rates (mrem/hr) reported for the tissue equivalent detectors shown on the first two sections of shielding berm are shown in the figure. Blank cells indicate variance exceeded 20% and are not reported.

### Residual dose rate on collimator

The effective dose rate for various irradiation and cooling times is provided in tabular form in the MARS.OUT output files and is reproduced here in Figure 28 for convenience. The results are also summarized in graphic form in Figure 29. The dose rate at 1 cm falls into the range of 10 to 100 mSv/hr (1 to 10 rem/hr) for medium term irradiation and cooling times.

IRRADIATIONTIME(day)=	0.5	1.0	5.0	30.0	100.0	365.0	7300.0
Tcool							
1sec	5.386E+01	5.857E+01	7.509E+01	1.000E+02	1.155E+02	1.355E+02	1.498E+02
1min	4.831E+01	5.301E+01	6.929E+01	9.443E+01	1.099E+02	1.299E+02	1.442E+02
10min	3.686E+01	4.152E+01	5.720E+01	8.291E+01	9.821E+01	1.184E+02	1.327E+02
0.5hr	2.790E+01	3.248E+01	4.748E+01	7.377E+01	8.893E+01	1.093E+02	1.235E+02
1hr	2.128E+01	2.573E+01	4.004E+01	6.689E+01	8.192E+01	1.024E+02	1.166E+02
2hr	1.508E+01	1.933E+01	3.270E+01	6.022E+01	7.510E+01	9.570E+01	1.099E+02
4hr	1.000E+01	1.391E+01	2.619E+01	5.437E+01	6.910E+01	8.985E+01	1.041E+02
6hr	7.761E+00	1.140E+01	2.294E+01	5.130E+01	6.590E+01	8.671E+01	1.009E+02
12hr	4.706E+00	7.816E+00	1.794E+01	4.639E+01	6.073E+01	8.167E+01	9.587E+01
1day	3.110E+00	5.616E+00	1.437E+01	4.194E+01	5.595E+01	7.699E+01	9.117E+01
2days	2.122E+00	3.972E+00	1.131E+01	3.681E+01	5.038E+01	7.141E+01	8.555E+01
7days	9.283E-01	1.811E+00	6.259E+00	2.500E+01	3.706E+01	5.756E+01	7.153E+01
30d	2.540E-01	5.036E-01	2.098E+00	1.031E+01	1.875E+01	3.653E+01	4.971E+01
0.5yr	3.905E-02	7.800E-02	3.761E-01	2.168E+00	5.355E+00	1.443E+01	2.373E+01
1yr	1.760E-02	3.516E-02	1.717E-01	1.004E+00	2.696E+00	7.862E+00	1.418E+01
2yr	6.506E-03	1.301E-02	6.401E-02	3.774E-01	1.064E+00	3.247E+00	6.349E+00
5yr	6.548E-04	1.309E-03	6.461E-03	3.821E-02	1.107E-01	3.482E+00	9.941E+00
10yr	7.220E-05	1.444E-04	7.193E-04	4.299E-03	1.379E-02	4.830E-02	3.163E-01
20yr	2.711E-05	5.423E-05	2.708E-04	1.623E-03	5.332E-03	1.917E-02	1.571E-01
30yr	1.643E-05	3.285E-05	1.641E-04	9.840E-04	3.254E-03	1.178E-02	1.074E-01

Figure 28: The contact dose rate in mSv/hr for the collimator for various irradiation and cooling times is reproduced from a MARS.OUT file. The irradiation intensity is 6.25E12 protons per second. The “cooling time in seconds” column has been omitted.

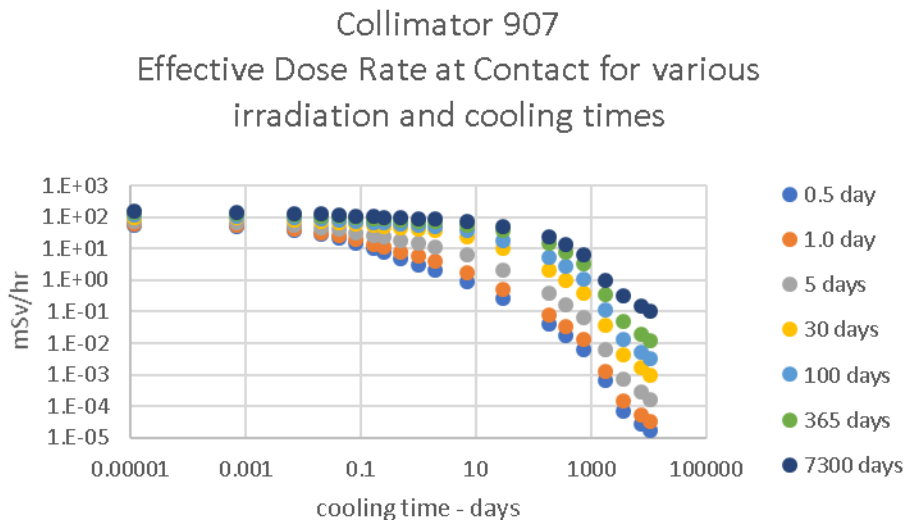
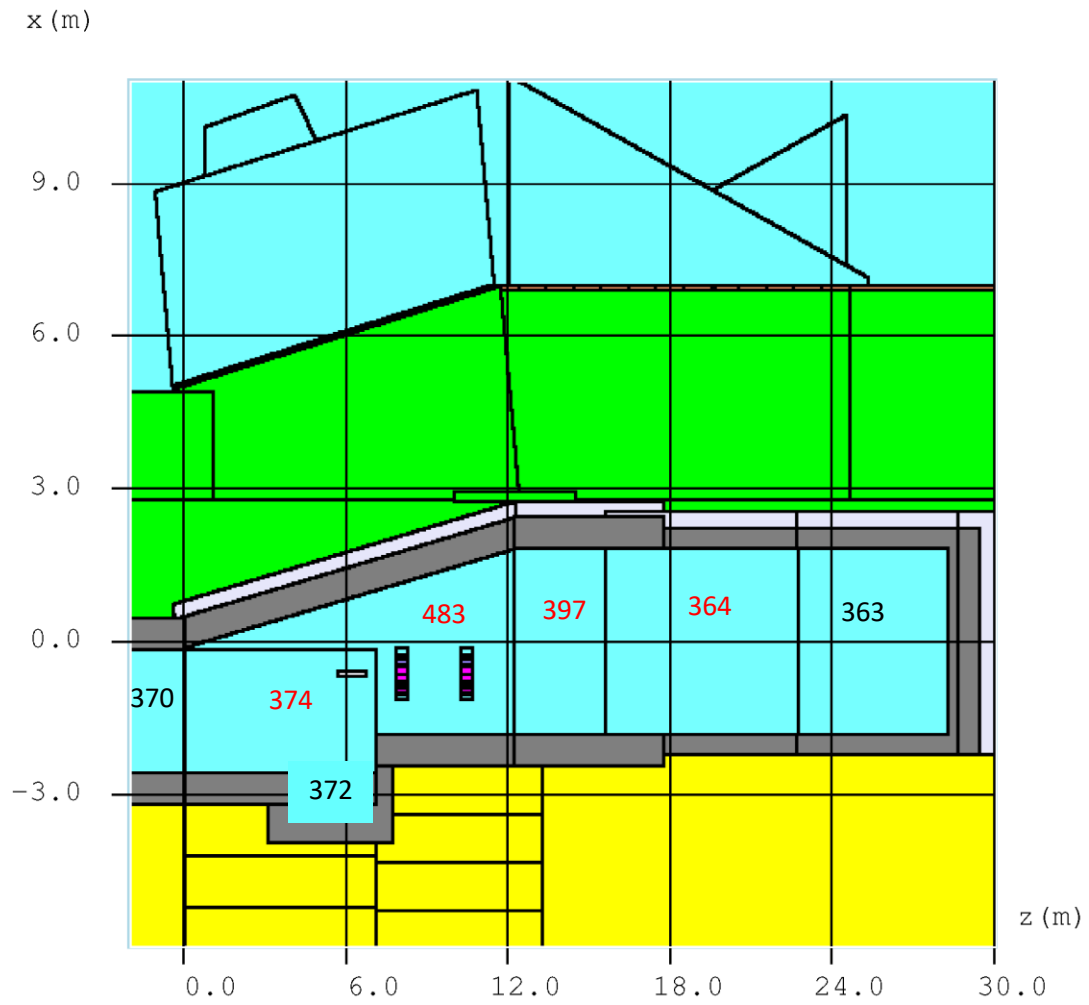


Figure 29: Tabular data from Figure 28 is repeated here is graphic form.

## Air Activation

The major air volumes of interest occur in the vicinity of the 907 collimator are shown in Figure 30. This information should be useful to determine if shielding the 907 collimator is necessary to reduce activated air emissions from the nearby monitored exhaust stack. The major contributor for airborne emissions at the M4 beam line exhaust stack will come from the Production Solenoid Room [21]. The contribution of air activation at the 907 collimator region will need to be included with that from other sources including the Production Solenoid Room.



x  
 ↗ z  
 x:z = 1: 1.8824; y0 = -120.0000 cm

Figure 30: This elevation view of the upstream tunnel region shows air volumes indicated with region numbers. As can be seen

Volume name	region number	Volume (cc)	hadron flux >30 MeV	% error (based upon star density)	hadron flux * volume	percent of contributing flux
APentair	370	1.67E+07	6.20E-10	2.4%	1.03E-02	0.1%
pitair	372	3.93E+06	1.63E-08	1.0%	6.43E-02	0.7%
sect1air	374	7.89E+07	4.29E-08	0.1%	3.39E+00	35.1%
uswalair	483	9.43E+07	4.82E-08	0.1%	4.55E+00	47.1%
stairent	398	6.12E+07	2.28E-09	0.6%	1.39E-01	1.4%
sect3air	397	6.43E+07	1.47E-08	0.3%	9.42E-01	9.8%
curve1a	364	8.26E+07	5.07E-09	0.4%	4.19E-01	4.3%
curve2a	363	6.48E+07	1.34E-09	0.8%	8.71E-02	0.9%
curve3a	362	1.02E+08	3.97E-10	1.1%	4.07E-02	0.4%
curve4a	361	4.68E+06	4.85E-11	11.2%	2.27E-04	0.0%
curve5a	360	1.71E+07	1.48E-11	10.3%	2.52E-04	0.0%
curve6a	359	1.03E+08	5.25E-12	7.5%	5.41E-04	0.0%
longsecta	358	3.86E+08	3.00E-11	1.7%	1.16E-02	0.1%
m5superai	357	8.10E+07	8.89E-13	15.8%	7.20E-05	0.0%
Totals:		1.16E+09			9.65E+00	100.0%
in weighted average hadron flux (hadron/cm2/p):					8.31E-09	

Table 3, about 95% of the air activation occurs within regions 364, 374, 397, and 483.

Volume name	region number	Volume (cc)	hadron flux >30 MeV	% error (based upon star density)	hadron flux * volume	percent of contributing flux
APentair	370	1.67E+07	6.20E-10	2.4%	1.03E-02	0.1%
pitair	372	3.93E+06	1.63E-08	1.0%	6.43E-02	0.7%
sect1air	374	7.89E+07	4.29E-08	0.1%	3.39E+00	35.1%
uswalair	483	9.43E+07	4.82E-08	0.1%	4.55E+00	47.1%
stairent	398	6.12E+07	2.28E-09	0.6%	1.39E-01	1.4%
sect3air	397	6.43E+07	1.47E-08	0.3%	9.42E-01	9.8%
curve1a	364	8.26E+07	5.07E-09	0.4%	4.19E-01	4.3%
curve2a	363	6.48E+07	1.34E-09	0.8%	8.71E-02	0.9%
curve3a	362	1.02E+08	3.97E-10	1.1%	4.07E-02	0.4%
curve4a	361	4.68E+06	4.85E-11	11.2%	2.27E-04	0.0%
curve5a	360	1.71E+07	1.48E-11	10.3%	2.52E-04	0.0%
curve6a	359	1.03E+08	5.25E-12	7.5%	5.41E-04	0.0%
longsecta	358	3.86E+08	3.00E-11	1.7%	1.16E-02	0.1%
m5uperai	357	8.10E+07	8.89E-13	15.8%	7.20E-05	0.0%
Totals:		1.16E+09			9.65E+00	100.0%
weighted average hadron flux (hadron/cm2/p):					8.31E-09	

Table 3: Air activation results for each of the model air volumes is listed in the table. 95% of the airborne activity is produced in 4 regions containing and just downstream of the 907 collimator.

### Groundwater activation

The distribution of groundwater activation in the glacial till beneath the 907 collimator and Q908/Q909 region is provided from the MTUPLE.EXG output file and is shown in Figure 31. The volumes containing about 99% of total stars include those volumes indicated in yellow/orange/red. The average star density obtained from the 99% volume is 1.28E-11 stars/cc/proton.

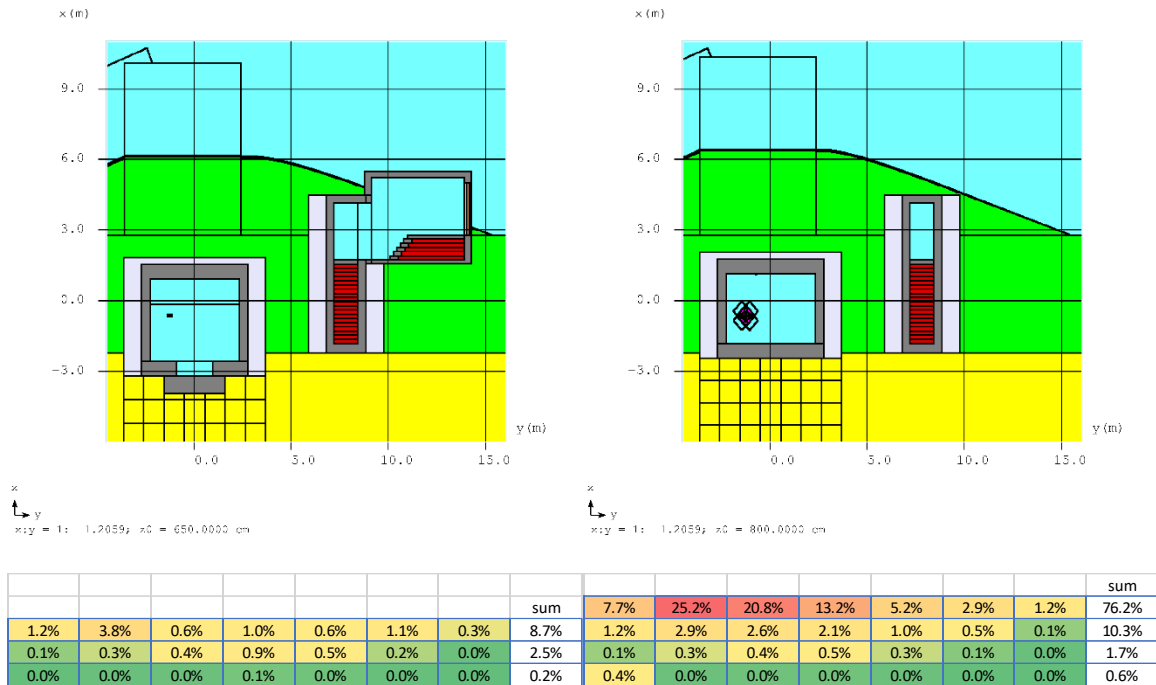


Figure 31: At top left is a cross section of tunnel showing the 21 ground water activation volumes below the floor in the vicinity of the platform lift pit. Region numbers are bottom left, 376; top left, 378; bottom right, 394; and top right, 396. At top right is a cross section of the tunnel showing 28 groundwater activation volumes beginning just after the step following the platform lift. Region numbers are bottom left, 455; top left, 458; bottom right, 479; and top right, 482. The longitudinal position of these two regions is illustrated in Figure 30. At bottom left, the total of groundwater activation is shown for the upstream region. At bottom right, the total is shown for the downstream region.

Groundwater activation is calculated from the method provided in Reference 17. As shown in Figure 32, using a 20 year irradiation time at  $6.25 \times 10^{12}$  protons/second, 2000 hours/year operation, ground water activation eventually reaches just over 1 ppm of the groundwater activation limit.

Mu2e Groundwater Calculations without Flushing (assuming no underdrains or sump pumps)								
	<sup>3</sup> H	<sup>22</sup> Na	S <sub>max</sub> toS <sub>ave</sub> =	0.019				
K(atom/star)=	0.075	0.02	dps-to-pCiPlus=	1.17E+06			<sup>3</sup> H	<sup>22</sup> Na
L=	0.9	0.135				Buildup	6.75E-01	9.95E-01
ρ(soil)=	2.25	2.25				t <sub>1/2</sub> (yr)=	12.33	2.602
w=	0.27	0.52	*Save(star/cc-p)=	1.28E-11		λ=	5.62E-02	2.66E-01
Factor-ave=	8.21E-19	2.51E-20				Decay=	3.25E-01	4.85E-03
			H-3_Hydro-xport R(Till)=	1.00E-09				
			Na22_Hydro-xport R(Till)=	1.00E-09				
			Tirr (yr) =	20				
			Tbeam-off (yr) =	20				
	Tritium			Sodium		After Year	Fraction of Total Limit in Aquifer	
Protons/year	C01 (pCi/cc-y)	C(t)f1 (pCi/cc-y)		C01 (pCi/cc-y)	C(t)f1 (pCi/cc-y)			
4.50E+19	3.69E+01	3.69E-08		1.13E+00	1.13E-09	1	6.52E-08	
4.50E+19	3.69E+01	3.69E-08		1.13E+00	1.13E-09	2	1.30E-07	
4.50E+19	3.69E+01	3.69E-08		1.13E+00	1.13E-09	3	1.96E-07	
4.50E+19	3.69E+01	3.69E-08		1.13E+00	1.13E-09	4	2.61E-07	
4.50E+19	3.69E+01	3.69E-08		1.13E+00	1.13E-09	5	3.26E-07	
4.50E+19	3.69E+01	3.69E-08		1.13E+00	1.13E-09	6	3.91E-07	
4.50E+19	3.69E+01	3.69E-08		1.13E+00	1.13E-09	7	4.56E-07	
4.50E+19	3.69E+01	3.69E-08		1.13E+00	1.13E-09	8	5.22E-07	
4.50E+19	3.69E+01	3.69E-08		1.13E+00	1.13E-09	9	5.87E-07	
4.50E+19	3.69E+01	3.69E-08		1.13E+00	1.13E-09	10	6.52E-07	
4.50E+19	3.69E+01	3.69E-08		1.13E+00	1.13E-09	11	7.17E-07	
4.50E+19	3.69E+01	3.69E-08		1.13E+00	1.13E-09	12	7.82E-07	
4.50E+19	3.69E+01	3.69E-08		1.13E+00	1.13E-09	13	8.48E-07	
4.50E+19	3.69E+01	3.69E-08		1.13E+00	1.13E-09	14	9.13E-07	
4.50E+19	3.69E+01	3.69E-08		1.13E+00	1.13E-09	15	9.78E-07	
4.50E+19	3.69E+01	3.69E-08		1.13E+00	1.13E-09	16	1.04E-06	
4.50E+19	3.69E+01	3.69E-08		1.13E+00	1.13E-09	17	1.11E-06	
4.50E+19	3.69E+01	3.69E-08		1.13E+00	1.13E-09	18	1.17E-06	
4.50E+19	3.69E+01	3.69E-08		1.13E+00	1.13E-09	19	1.24E-06	
4.50E+19	3.69E+01	3.69E-08		1.13E+00	1.13E-09	20	1.30E-06	

Figure 32: Using the average star density for the 99% activation volume, and assuming  $4.5 \times 10^{19}$  protons per year, the ground water activation level eventually reaches just over 1 ppm of the groundwater activation limit.

## Surface water activation

Surface water produced near the 907 collimator is collected by a collection system which is routed to the Main Ring Pond and on-site collection/storage system. There is no observable unique surface water discharge point near the 907 collimator. The surface water activation is calculated from Reference 17. As shown in Figure 33, applying the average star density from the groundwater result for the surface water activation calculation results in surface water activation well below surface discharge limits for any conceivable sump pumping frequency.





												TOTAL TLM Response	1836.2664
	reg #	volume	energy dep	error	%error	ev/IP	e per nC	protons/s	s/m	e per IP	ev/GeV	nC/min	nC/E10 p
1detgas	99	3.00E+02	6.82E-15	6.84E-16	10.0%	30	6.24E+09	6.25E+12	60	1	1.00E+09	4.1	0.0390
1detgas	100	3.00E+02	1.19E-14	1.13E-15	9.4%	30	6.24E+09	6.25E+12	60	1	1.00E+09	7.2	0.0683
1detgas	101	3.00E+02	2.50E-14	3.73E-15	14.9%	30	6.24E+09	6.25E+12	60	1	1.00E+09	15.0	0.1431
1detgas	102	3.00E+02	4.83E-14	5.37E-15	11.1%	30	6.24E+09	6.25E+12	60	1	1.00E+09	29.0	0.2766
1detgas	103	3.00E+02	1.21E-13	8.91E-15	7.4%	30	6.24E+09	6.25E+12	60	1	1.00E+09	72.7	0.6926
1detgas	104	3.00E+02	3.02E-13	9.47E-15	3.1%	30	6.24E+09	6.25E+12	60	1	1.00E+09	181.5	1.7285
1detgas	105	3.00E+02	4.88E-13	1.38E-14	2.8%	30	6.24E+09	6.25E+12	60	1	1.00E+09	293.0	2.7908
1detgas	106	3.00E+02	4.14E-13	1.34E-14	3.2%	30	6.24E+09	6.25E+12	60	1	1.00E+09	248.6	2.3679
1detgas	107	3.00E+02	3.95E-13	6.45E-14	16.3%	30	6.24E+09	6.25E+12	60	1	1.00E+09	237.6	2.2631
1detgas	108	3.00E+02	2.36E-13	8.95E-15	3.8%	30	6.24E+09	6.25E+12	60	1	1.00E+09	141.8	1.3508
1detgas	109	3.00E+02	1.88E-13	9.72E-15	5.2%	30	6.24E+09	6.25E+12	60	1	1.00E+09	113.1	1.0772
1detgas	110	3.00E+02	1.61E-13	1.16E-14	7.2%	30	6.24E+09	6.25E+12	60	1	1.00E+09	97.0	0.9238
											total	1440.8	13.7216
2detgas	144	3.28E+02	1.14E-13	5.78E-15	5.1%	30	6.24E+09	6.25E+12	60	1	1.00E+09	75.1	0.7150
2detgas	145	3.28E+02	1.01E-13	3.65E-15	3.6%	30	6.24E+09	6.25E+12	60	1	1.00E+09	66.3	0.6318
2detgas	146	3.28E+02	8.66E-14	2.75E-15	3.2%	30	6.24E+09	6.25E+12	60	1	1.00E+09	56.9	0.5416
											total	198.3	1.8885
3detgas	174	2.98E+02	8.50E-14	3.87E-15	4.6%	30	6.24E+09	6.25E+12	60	1	1.00E+09	50.7	0.4829
3detgas	175	2.98E+02	7.17E-14	4.67E-15	6.5%	30	6.24E+09	6.25E+12	60	1	1.00E+09	42.8	0.4074
3detgas	176	2.98E+02	5.08E-14	2.23E-15	4.4%	30	6.24E+09	6.25E+12	60	1	1.00E+09	30.3	0.2885
3detgas	177	2.98E+02	3.78E-14	2.54E-15	6.7%	30	6.24E+09	6.25E+12	60	1	1.00E+09	22.5	0.2147
3detgas	178	2.98E+02	2.21E-14	8.87E-16	4.0%	30	6.24E+09	6.25E+12	60	1	1.00E+09	13.2	0.1254
3detgas	179	2.98E+02	1.49E-14	7.13E-16	4.8%	30	6.24E+09	6.25E+12	60	1	1.00E+09	8.9	0.0848
3detgas	180	2.98E+02	9.91E-15	6.92E-16	7.0%	30	6.24E+09	6.25E+12	60	1	1.00E+09	5.9	0.0563
											total	174.3	1.6602
4detgas	213	2.69E+02	1.72E-14	7.90E-15	46.0%	30	6.24E+09	6.25E+12	60	1	1.00E+09	9.2	0.0881
4detgas	214	2.69E+02	6.29E-15	4.16E-16	6.6%	30	6.24E+09	6.25E+12	60	1	1.00E+09	3.4	0.0323
4detgas	215	2.69E+02	4.78E-15	2.85E-16	6.0%	30	6.24E+09	6.25E+12	60	1	1.00E+09	2.6	0.0245
4detgas	216	2.69E+02	4.29E-15	4.65E-16	10.8%	30	6.24E+09	6.25E+12	60	1	1.00E+09	2.3	0.0220
4detgas	217	2.69E+02	3.77E-15	2.98E-16	7.9%	30	6.24E+09	6.25E+12	60	1	1.00E+09	2.0	0.0193
4detgas	218	2.69E+02	2.74E-15	2.20E-16	8.0%	30	6.24E+09	6.25E+12	60	1	1.00E+09	1.5	0.0140
											total	21.0	0.2004
5detgas	234	2.55E+03	1.78E-15	1.26E-16	7.1%	30	6.24E+09	6.25E+12	60	1	1.00E+09	9.1	0.0864
6detgas	240	1.98E+03	2.70E-16	3.24E-17	12.0%	30	6.24E+09	6.25E+12	60	1	1.00E+09	1.1	0.0102
7detgas	246	1.83E+03	6.88E-17	1.11E-17	16.2%	30	6.24E+09	6.25E+12	60	1	1.00E+09	0.3	0.0024
8detgas	252	3.26E+03	8.16E-17	6.18E-17	75.7%	30	6.24E+09	6.25E+12	60	1	1.00E+09	0.5	0.0051
											Total nC/E10 p	15.7141	

Figure 34: The TLM response is calculated from the energy deposition in the argon/CO<sub>2</sub> detector gas for the 8 lengths of TLM detector cable. Most of the total detector response results from the downstream half of the first detector. The total calculated detector response is about 1800 nC/minute.

## Analysis and Discussion

The prompt effective dose rate on the M4 beam line shielding berm resulting from the 0.28% normal beam loss on the 907 collimator is up to about 0.5 mrem/hr (see Figure 19 through Figure 23 and Figure 27). The FRCM [20] requirements for posting radiological areas are reproduced in Figure 35 and Figure

36 for convenience. For the normal case, the requirement is to post the shielding berm with Controlled Area signs and to limit occupancy to one hour. To fulfill these requirements, installation of a fence would be a practical method to attach the necessary signs and to permit enforcement of the 1 hour occupancy limit.

The effective dose rate at the exit stairway given in Table 2 is 32 urem/hr. The only additional requirement would be to post the exterior of the exit door with the Exclusion Area posting.

The effective dose rate downstream of the M5 shield wall given in Table 2 is <1 urem/hr. No posting of the region would be required due to normal beam loss on the 907 collimator. However, other more severe beam loss potential will exist due to losses downstream of the 907 collimator which may require posting and additional control measures.

Dose Rate (DR) Under Normal Operating Conditions	Controls
All interlocked doors or gates leading from non-enclosures into an interlocked Exclusion Area	Signs (EXCLUSION AREA – No Access Permitted with Beam Enabled.)
DR < 0.05 mrem/hr	No precautions needed.
$0.05 \leq \text{DR} < 0.25$ mrem/hr	Signs (CAUTION -- Controlled Area). No occupancy limits imposed.
$0.25 \leq \text{DR} < 5$ mrem/hr	Signs (CAUTION -- Controlled Area) and minimal occupancy (occupancy duration of less than 1 hr).
$5 \leq \text{DR} < 100$ mrem/hr	Signs (CAUTION -- Radiation Area) and rigid barriers (at least 4' high) with locked gates. For beam-on radiation, access restricted to authorized personnel. Radiological Worker Training required.
$100 \leq \text{DR} < 500$ mrem/hr	Signs (DANGER -- High Radiation Area) and 8 ft. high rigid barriers with interlocked gates or doors and visible flashing lights warning of the hazard. Rigid barriers with no gates or doors are a permitted alternate. No beam-on access permitted. Radiological Worker Training required.
DR $\geq$ 500 mrem/hr	Prior approval of SRSO required with control measures specified on a case-by-case basis.

Figure 35: FRCM Table2-6 Control of Accessible Accelerator/Beamline Areas for Prompt Radiation Under Normal Operating Conditions (refer to Article 236.2(b))

Maximum Dose (D) Expected in 1 hour	Controls
All interlocked doors or gates leading from non-enclosures into an interlocked Exclusion Area	Signs (EXCLUSION AREA – No Access Permitted with Beam Enabled.)
$D < 1$ mrem	No precautions needed.
$1 < D \leq 10$ mrem	Minimal occupancy only (duration of credible occupancy $< 1$ hr) no posting
$1 \leq D < 5$ mrem	Signs (CAUTION -- Controlled Area). No occupancy limits imposed. Radiological Worker Training required.
$5 \leq D < 100$ mrem	Signs (CAUTION -- Radiation Area) and minimal occupancy (duration of occupancy of less than 1 hr). The assigned RSO has the option of imposing additional controls in accordance with Article 231 to ensure personnel entry control is maintained. Radiological Worker Training required.
$100 \leq D < 500$ mrem	Signs (DANGER -- High Radiation Area) and rigid barriers (at least 4' high) with locked gates. For beam-on radiation, access restricted to authorized personnel. Radiological Worker Training required.
$500 \leq D < 1000$ mrem	Signs (DANGER -- High Radiation Area) and 8 ft. high rigid barriers with interlocked gates or doors and visible flashing lights warning of the hazard. Rigid barriers with no gates or doors are a permitted alternate. No beam-on access permitted. Radiological Worker Training required.
$D \geq 1000$ mrem	Prior approval of SRSO required with control measures specified on a case-by-case basis.

Figure 36: FRCM Table2-7 Control of Accessible Accelerator/Beamline Areas for Prompt Radiation Under Accident Conditions When It is Likely that the Maximum Dose Can Be Delivered (See Article 236.2 b for more details)

TLM response due to normal losses on the 907 collimator is calculated at about 1,800 nC/min. A TLM system trip level of 3,000 nC/min would permit operation with the 0.28% beam loss and leave some additional operating space above the trip level. The effective dose rates reported above could increase by 40%, but would remain with the cited posting and access requirements for the normal condition. This trip level would simultaneously limit the accident condition to the upper limit of the normal condition. Figure 36 shows the FRCM requirements for the accident condition; no additional posting or access requirements would be imposed with a TLM system trip level of 3,000 nC/min.

As shown in Figure 32 and Figure 33, ground water and surface water activation remain well within their respective limits due to normal operational beam loss on the 907 collimator.

The air activation estimated for normal beam loss at the 907 collimator will eventually need to be considered as an additional emissions source along with that originating in the Production Solenoid

room [21], the AC dipole, and any additional collimators located further downstream in the M4 beam line.

The residual dose rate on the 907 collimator calculated for nominal operating conditions, e.g., 30 days irradiation, 1 day cooling will be significant. Personnel access in the vicinity of the 907 collimator and aisleway will be limited due to high radiation levels, perhaps several hundred mrem/hr or more.

## Supplemental shielding

While not absolutely necessary, the inclusion of sufficiently thick supplemental steel shielding around the collimator would have significant benefits including:

- Reduction in radiation effective dose rates on the shielding berm. Each foot of steel shielding placed above the 907 collimator could reduce dose rates on the shielding berm by up to a factor of 10.
- Reduction in fencing and posting requirements on the shielding berm above the 907 collimator
- Reduction in TLM response during normal beam operation which would provide additional operating margin. This could be especially important if other unknown/unspecified beam losses eventually contribute to TLM response.
- Reduction in air activation due to reduction of hadron flux in air
- Reduction of effective dose rate at the exit stairway door.
- Reduction in personnel radiation exposure in the vicinity of the 907 collimator and aisleway during M4 enclosure access

The benefit that supplemental steel shielding can provide is strongly dependent upon the available space for its installation above, below, and at either side of the 907 collimator.

## Summary

A MARS simulation has been produced which provides estimates of radiation protection parameters due to normal beam loss on the 907 collimator. The inclusion of non-trivial layers of supplemental steel shielding should significantly reduce effective dose rates on the shielding berm, reduce fencing and posting requirement, reduce air activation, and provide additional operating margin by reducing TLM response due to normal losses on the 907 collimator. A subsequent MARS simulation should be made to quantify these improvements if/when a shielding plan for the 907 collimator becomes available.

## References

1. N.V. Mokhov and C.C. James, "The Mars Code System User's Guide, Version 15 (2016)", Fermilab-FN-1058-APC (2017); <https://mars.fnal.gov><http://www-ap.fnal.gov/MARS/>.
2. Muon Campus Preliminary Shielding Assessment, Beamsdoc.db4513-v7, A. Leveling, June 1, 2015
3. M4 Beamline Project 6-10-22 As Built Drawings, [file:///Blue1/FESS/FESS Archive/6/10/22/ AsBuilt%20Drawings%20&%20PDFs/6-10-22/](file:///Blue1/FESS/FESS%20Archive/6/10/22/AsBuilt%20Drawings%20&%20PDFs/6-10-22/)
4. Particle Splitting/Branching Provision in MARS15 of August 2017, Igor Tropin, MARS Meeting–FNAL, August 11, 2017

5. CA-7 density reported by Tom Hamernick in email correspondence, February 29,2016
6. M4 beamline site coordinates, file (m4\_sag\_corrected\_mtxt) provided by Jerry Annala, 1/7/19
7. Total Loss Monitor Response as a function of Particle Fluence, Beams doc.db 4559-v1, A. Leveling, September 30,2014
8. FRCM Chapter 2-Radiological Standards FINAL ESHQ Doc.db Document 444-v15, February 2, 2018
9. Chipmunk and TLM radiation detector trip calculators, Beams doc.db 4732-v3, A. Leveling, May 6,2016
10. Proton beam source file provided by V. Nagaslaev, via Dropbox, April 1, 2019
11. CH-1 Mu2e Collimator Assembly with Extension drawing, F10070611 and others, provided by D. Still, March 12, 2019
12. Extinction Collimator #1 — Info for T. Leveling for MARS calculation, Dean Still ,3/11/19
13. Private communication, Dirk Hurd to Dean Still, March 18, 2019
14. Private communication, N. Mokhov, April 5, 2019
15. Private communication, J. Morgan, November 18, 2016.
16. Private communication, V. Nagaslaev, April 10, 2019
17. Groundwater and Surface Water Calculation Worksheet, K. Vaziri, 6/14/19
18. TLM and Chipmunk Response Check for 400 MeV beam loss at Booster, A. Leveling, Beams doc.db 5170-v1, June 1, 2016
19. Comparison of 3 TLM Detector Responses in Parallel and Series Arrangements, A. Leveling, Beams doc.db 4549-v1, February 28, 2014
20. FRCM Chapter 2 - Radiological Standards FINAL, ESHQ Doc.db Document 444-v15, February 2, 2018
21. Mu2e Radioactive Air Emissions Estimates Study, MU2E DocDB Document 5739-v4, K. Vaziri, July 8, 2015